

Technical Report No: ND06 - 03

**MODELING GROUNDWATER DENITRIFICATION
BY FERROUS IRON USING PHREEQC**

by

**Tedros Tesfay
Scott Korom**

**Dept. of Geology and Geological Engineering
University of North Dakota
Grand Forks, North Dakota**

November 2006

**North Dakota Water Resources Research Institute
North Dakota State University, Fargo, North Dakota**

Technical Report No: ND06-3

**MODELING GROUNDWATER DENITRIFICATION
BY FERROUS IRON USING PHREEQC**

by

Tedros Tesfay¹
Scott Korom²

**WRI Graduate Research Fellow¹ and Associate Professor²
Department of Geology and Geological Engineering
University of North Dakota
Grand Forks, ND 58202**

November 2006

The work upon which this report is based was supported in part by federal funds provided by the United States of Department of Interior in the form of ND WRI Graduate Research Fellowship for the graduate student through the North Dakota Water Resources Research Institute.

Contents of this report do not necessarily reflect the views and policies of the US Department of Interior, nor does mention of trade names or commercial products constitute their endorsement or recommendation for use by the US government.

**Project Period: March 1, 2003 – August 31, 2006
Project Number: 2003ND27B**

**North Dakota Water Resources Research Institute
Director: G. Padmanabhan
North Dakota State University
Fargo, North Dakota 58105**

TABLE OF CONTENTS

<i>LIST OF FIGURES</i>	4
<i>LIST OF TABLES</i>	6
<i>ABSTRACT</i>	7
I. INTRODUCTION AND OBJECTIVES	8
II. REGIONAL GEOLOGY	11
The Field Sites	11
Robinson (North Dakota)	11
Karlsruhe-S (North Dakota)	12
Akeley (Minnesota)	12
III. IRON GEOCHEMISTRY AND DENITRIFICATION	13
IV. ANALYTICAL METHODS AND RESULTS	16
Ferrous Iron Analytical Methods and Results	18
Chemical Extraction	18
X-ray Diffraction	18
Mössbauer Spectroscopy	25
V. GEOCHEMICAL MODELING METHODS	31
Forward Reaction Modeling	33
Modeling Input data: Initial Solution	33
Dilution	33
Cation Exchange Processes	34
Reversible Reactions	35
Redox Reactions	35
VI. GEOCHEMICAL MODELING RESULTS	37

Modeled vs. Measured Cations and Anions	37
Control Chamber (C-ISM)	37
Nitrate Chamber (N-ISM)	40
VII. CONCLUSIONS	46
<i>ACKNOWLEDGMENTS</i>	47
<i>REFERENCES</i>	47

LIST OF FIGURES

Figures	Page
1. Map of North Dakota and Minnesota Showing Locations of the Study Sites	10
2. Iron Cycle in Environmental Biogeochemistry	15
3. Texture Analyses of Aquifer Sediments for Akeley (MN), Robinson (ND) and Karlsruhe-S (ASTM Methodology)	17
4. Results of Wet Chemical Extraction (Ferrous Iron), High Combustion Method (Organic Carbon Analyzer) and Chromium Reduction Method (Sulfide) for Akeley (MN), Robinson (ND) and Karlsruhe-S	20
5. XRD Scan of Aquifer Sediment Sample from Akeley, MN	22
6. XRD Scan of Aquifer Sediment Sample from Karlsruhe-S, ND	23
7. XRD Scan of Aquifer Sediment Sample from Robinson, ND	24
8. Ranges of Isomer Shifts (δ) for Iron Compounds of Different Oxidation and Spin States and how Isomer Shift (δ) and Quadrupole Splitting (ΔE_Q) are measured from the Mossbauer spectrum	26
9. Mössbauer Spectroscopy Measurements of Aquifer Sediment Sample for Akeley, MN (Colorado School of Mines)	28
10. Mössbauer Spectroscopy Measurements of Aquifer Sediment Sample for Karlsruhe-S (ND) (Dalhousie University Halifax)	29
11. Mössbauer Spectroscopy Measurements of Aquifer Sediment Sample for Robinson (ND) (Dalhousie University Halifax)	30
12. Forward Reaction Modeling Conceptual Representation for Control and Nitrate Chambers	32
13. Modeled (broken line) vs. Measured (solid line) Cations (A) and Anions (B), Robinson Control chamber	38
14. Modeled (broken line) vs. Measured (solid line) Cations (A) and Anions (B), Akeley Control chamber	39

15. Average Contribution of Each Electron Donor in the Natural Denitrification Reactions of North Dakota and Minnesota Aquifers, as Computed via Advanced Geochemical Modeling, PHREEQC; Employing the Concept of Partial Geochemical Modeling (Akeley, Robinson and Karlsruhe-S)	41
16. Modeled (broken line) vs. Measured (solid line) Cations (A) and Anions (B), Robinson Nitrate chamber	43
17. Modeled (broken line) vs. Measured (solid line) Cations (A) and Anions (B), Karlsruhe-S Nitrate chamber	44
18. Modeled (broken line) vs. Measured (solid line) Cations (A) and Anions (B), Akeley Nitrate chamber	45

LIST OF TABLES

Table	Page
1. Geochemical Analyses of Organic Carbon, Pyrite and Ferrous Iron for Akeley (MN), Robinson (ND) and Karlsruhe-S	19
2. XRD Measurements of the Major Minerals for Akeley (MN), Robinson (ND) and Karlsruhe-S	21
3. Mössbauer Spectroscopy Measurements of Aquifer Sediments for Akeley (MN), Robinson (ND) and Karlsruhe-S (Department of Physics and Atmospheric Science Dalhousie University Halifax, Nova Scotia Canada)	25
4. Replicate Mössbauer Spectroscopy Measurements of Aquifer Sediments for Akeley (MN), Robinson (ND) and Karlsruhe-S (Colorado School of Mines)	25
5. Relative Roles of the Common Reductants in Aquifer Denitrification Reactions for Akeley (MN), Robinson (ND) and Karlsruhe-S (ND)	40

ABSTRACT

Nitrate is one of the most common groundwater contaminants, and ingesting it leads to potential health risks. Denitrification, the only effective process to eliminate nitrate, is limited by the abundance of biologically available electron donors. Thus, understanding the natural denitrification capacity of aquifers, through the analysis of all the major electron donors, is essential.

A better way to estimate groundwater denitrification reactions is to compute the mass balance of the redox sensitive species. The University of North Dakota (UND) denitrification team installed mesocosms (ISMs) to understand the fate of nitrate in field conditions. Accordingly, the team has shown the significant role of sulfides (dominantly pyrite) and organic carbon in the denitrification processes of the regional aquifers. However, the role of Fe(II) has largely been overlooked in regional studies mainly because of two reasons: 1) the geochemical evidence for ferrous iron is more difficult to decipher due to the precipitation of Fe(III)-oxyhydroxides from the aqueous solution. 2) in the event when denitrification by both Fe(II) and organic carbon gave rise to precipitating reaction products, the role of Fe(II) is deceptively masked by that of the organic carbon. Thus far, little is known about the significance of solid phase biologically available ferrous iron in our region. We hypothesized that Fe(II)-supported denitrification, owing to the abundance of iron in aquifer sediments, has regional environmental significance.

Three techniques, wet chemical extraction, x-ray diffraction and Mössbauer spectroscopic measurements, were combined to determine ferrous iron contents and Fe(II)-bearing minerals of aquifer sediments. Geochemical modeling (PHREEQC) was employed to get an insight into the in situ denitrification processes that take place via all the common electron donors. Emphasis was given to Fe(II)-supported denitrification reactions because it has been overlooked in our region.

All aqueous analytical data, mineralogy and chemistry of sediments and geochemical modeling work support the research hypothesis. As a result, all the major electron donors are found to be important and Fe(II)-supported denitrification appears to have a significant role as a natural remediation process in the aquifers of our region.

Introduction and Objectives

Aquifers are important sources of drinking water in many parts of the world (Fetter, 1994). Groundwater serves as the primary domestic water supply for over 90% of the rural population, and 50% of the total population of North America (Power and Schepers, 1989). Groundwater pollution has grown in the last 100 years (McKeon et al., 2005 and references therein) and nitrate is one of the most common groundwater contaminants (Gillham and Cherry, 1979). Agricultural activities are the major cause of anthropogenic point sources (septic tanks, and dairy lagoons, etc.) and non-point sources (fertilizers, manure, and leguminous crops, etc.) of nitrate contamination (Rodvang and Simpkins, 2001). In the United States the use of nitrogen in commercial fertilizer increased from 1945 to 1993 by about twenty-fold (Rodvang and Simpkins, 2001).

An elevated concentration of nitrate cause some health problems such as methemoglobinemia in infants (Afzal, 2006), while the relationship between ingested excess nitrates and deadly diseases, such as stomach cancer and negative reproductive outcomes in adults, is debatable (Manassaram et al., 2006). Once groundwater is contaminated, the cost of protecting consumers from excess nitrate health risks is high. Moreover, conventional drinking water treatment processes, performed at water supply plants or in homes, such as ion exchange, reverse osmosis, and electrodialysis are expensive (EPA website: www.epa.gov/OGWDW/methods/inch_tbl.html). Hence, after the U.S. Congress passed the Safe Drinking Water Act in 1974, the Environmental Protection Agency (EPA) set a drinking water maximum contaminant level of 10 mg/L for nitrate-nitrogen.

Nitrate contamination is of particular concern in unconfined aquifers beneath intensive agricultural activities. Aquifers of glacial origin are among them and if they have moderate to high hydraulic conductivity, nitrate leaches to the water table easily (Rodvang and Simpkins, 2001). Examples of such aquifers are located in the upper Midwest, including Minnesota and North Dakota. Other hydrogeologic factors that affect nitrate contamination include depth to water, sediment texture, net recharge, topography, etc. (Puckett and Cowdery, 2002). Using these factors researchers have attempted to make aquifer nitrate vulnerability indices; however, the indices largely ignore the geochemical characteristics (reduction capacity) of aquifers (Korom, 2005).

Denitrification is the only effective process that converts significant amounts of nitrate irreversibly into harmless nitrogen gas in groundwater environments (Korom, 1992 and references therein). It is a natural process that requires an anaerobic environment, denitrifying bacteria, and sufficient and reactive electron donating species (Firestone, 1982). Numerous studies show that the availability of electron donors limits the denitrification potential of aquifers (Trudell et al., 1986; Korom, 1992; Starr and Gillham, 1993; Robertson et al., 1996). Hence, knowledge of the natural denitrification capacity of aquifers, through the analysis of electron donors, is required to manage the ongoing nitrate load into groundwater systems.

The most common electron donors are organic carbon, inorganic sulfides (dominantly pyrite), ferrous iron, and possibly manganese. However, the natural occurrence of

manganese is 5 - 10 times less than that of iron (Appelo and Postma, 1996) and will not be considered further. The UND Denitrification research team has shown that organic carbon and sulfides are active electron donors in North Dakota and Minnesota aquifers (Korom et al., 2005). However, the role of Fe(II) has largely been overlooked in the regional studies mainly because of the difficulty of measuring Fe(II)-supported denitrification reactions from the ISM analyses. The study of the significance of Fe(II) becomes more complicated when organic carbon-supported denitrification gives precipitating reaction products. Thus far, little is known about the regional significance of solid phase, biologically available ferrous iron in the reduction of nitrates from groundwater. In glaciated formations that have complex geological and geomorphological (depositional and subsequent events) histories, such as the aquifers of this region, a variety of electron donors may contribute to denitrification (Hartog et al., 2005). Our contention was that Fe(II), owing to its abundance, plays a significant role in regional aquifer denitrification processes.

When studying Fe(II) the two inseparable issues that needed to be addressed were the abundance of ferrous iron and its role in the denitrification processes. Hence, determining the solid phase Fe(II) content of the sediments at the research sites, through x-ray diffraction (XRD), Mössbauer spectroscopy and wet chemical extractions, was the first objective of my project. In addition, solid phase inorganic sulfides (dominantly pyrite) and organic carbon contents were also measured to estimate the total denitrification capacity of the sediments at the research sites.

The second objective was to verify the significance of Fe(II)-mineral species in the natural reduction of excess nitrates from groundwater. Unlike sulfides, the roles of Fe(II) and organic carbon are complicated by the subsequent precipitation of the denitrification reaction products, namely Fe(III)-oxyhydroxides and inorganic carbon, respectively (Korom et al., 2005). A method was developed to help resolve the issue by estimating the upper limit of the amount of inorganic carbon that could be precipitated with the use of the geochemical modeling program, PHREEQC (Parkhurst and Appelo, 1999). Then, by process of elimination the role of Fe(II)-supported denitrification would be determined. The forward geochemical modeling intends to mimic the most common aquifer reactions, cation exchange, reversible reactions (dissolution and precipitation of minerals), and redox reactions. The effect of mixing on the tracer ions was corrected before simulating the analytical data.

This study focused on seven sites (Fig 1). The Akeley (MN), Robinson (ND) and Karlsruhe-S (ND) sites, where organic carbon and inorganic sulfides did not seem to be the dominant electron donors supporting denitrification (Korom, 2005). The remaining four sites are presented concisely in the appendices. The Hamar (ND) and Karlsruhe-G (ND) ISMs were omitted because little to no denitrification was measured at these sites (Korom, 2005).



Figure 1. Map of North Dakota and Minnesota Showing Locations of the Study Sites.

Regional Geology

Groundwater occurs in the various rocks that form the Earth's crust and thus is directly or indirectly affected by the surrounding geology. Generally, the geology of the region comprises crystalline rocks of Precambrian age, stratified sedimentary rocks, and glacial drift (Stoner et al., 1993). The Precambrian rocks of Minnesota found close to and sometimes at the surface are primary igneous and metamorphic rocks (Heath, 1984). The Precambrian rocks in North Dakota are under extensive deposits of water-bearing sedimentary formations. Many of them lie over the older units and are dominantly sandstone, limestone, and dolomite. However, these formations gradually thin eastward (Stoner et al., 1993). Thus, the bedrock in much of Minnesota is overlain by thin soils derived primarily from weathering of the basement rocks (Heath, 1984).

Minnesota and North Dakota aquifers resulted primarily from glacial processes that affected the surficial geology and geomorphology of the region. The glaciations in the central region of the U.S. occupy an area of 13 million km² extending from the Triassic Basin in Connecticut and Massachusetts and the Catskill Mountains in New York on the east to the northern part of the Great Plains in Montana on the west. Their ages range from Pre-Illinoian (> 500 Ka B.P.) to the late Wisconsinan (~10 ka B.P.) (Rodvang and Simpkins, 2001 and references therein). The thickness of the glacial-drift that covers the research sites ranges from 0 to 600 feet, but is generally 150 to 300 feet thick (Stoner et al., 1993). The lithology of the glacial-drift is unsorted and unconsolidated mixtures of clay, silt, sand, gravel, and boulders (Stoner et al., 1993). Shale, which is expected to have the three important electron donors, organic carbon, sulfides and ferrous iron, occurs in some places, mainly among the thick glacial-drift layers (Schultz et al. 1980). The local differences among the composition of the regional aquifers arise mainly from subsequent depositional and erosional processes. Hartog et al. (2005) explained that in variable degrees of importance, the depositional environment of the sediment, the occurrence of subsequent sediment reworking, and paleohydrological conditions are all important factors that may affect the relative abundance and reactivity of sedimentary reductants. The authors (Hartog et al., 2005) further explained that sedimentary organic carbon is also important because its anaerobic degradation causes the diagenetic formation of reactive Fe(II), Mn(II), and sulfides.

The Field Sites

Robinson (North Dakota)

The Robinson site is in glacial outwash sediments of the Kidder County aquifer complex (Bradley et al., 1963). The depth of the ISMs, which were installed in 2000, extends from 22 ft to 27 ft. They are located at T. 143 N, R. 71 W, section 29CCD (see location format definition at www.swc.state.nd.us/dbase/locatfmthelp.html). Two tracer tests have been completed in the Robinson ISMs, but only the results of the first tracer test were available in time for this study. Well logs of aquifer cores taken by North Dakota State Water Commission (NDSWC) close to these ISMs indicate that fine to coarse brown (oxidized) sand dominates the first 11 ft, which is then followed by fine to coarse gray (unoxidized) sand up to the depth of 40 ft below the surface (<http://www.swc.state.nd.us>).

Karlsruhe-S (North Dakota)

The Karlsruhe-S site is near the Wintering River, McHenry County, North Dakota, in the sand and gravel deposits of the Karlsruhe aquifer. It was installed in the summer of 2003. The depth of Karlsruhe-S ISM extends from 16 ft to 21 ft. The Karlsruhe-S site is located at T. 154 N, R. 77 W, section 33DDD. Two tracer tests were completed in this site but only the data from the first tracer test (Warne, 2004; Spencer, 2005) were available for this project. Well logs close to the Karlsruhe-S ISM, indicate the presence of alternate layers of fine to medium grain sand, silt, clay and some lignite. It also shows that the formation is dominantly gley (reduced) in color. Furthermore, the NDSWC well log database indicates that the aquifer is dominated by sand and gravel composed of silicates, carbonates and some lignite for the first 21 ft below the surface (NDSWC website: <http://www.swc.state.nd.us>).

Akeley (Minnesota)

The Akeley site (MN) is near the Shingobee River in proglacial fluvial sediment deposited over stagnant glacial ice (Mooers and Norton, 1997). The site is located at 46° 59' 00'' N – 96° 11' 26'' W. The ISMs were installed in 2001 at a depth extending from 15 to 20 ft. The Akeley site and two other sites (Perham-M and Perham-W in the west central of Minnesota) are close in proximity and the prevailing mineralogy determined through this project is consistent with that in previously published papers. Zachara et al. (2004), using various advanced analytical instruments, explained that the mineralogy of this region is mixed among carbonate (sedimentary), igneous and metamorphic provenances. Puckett and Cowdery (2002) and Tuccillo et al., (1999) indicated that quartz, plagioclase feldspar, alkali feldspar, calcite, and dolomite are the dominant minerals. In the finer fraction (< 1 μm) chlorite (clinochlore) and kaolinite, hornblende, and some other clay minerals were also observed (Puckett and Cowdery, 2002). The bulk mineralogy analyses also demonstrate that clinochlore and kaolinite and amphibole (hornblende) minerals exist as accessory minerals. Total solid organic carbon, found by the above authors, ranges from 0.01% to 1.45%. Examination of sediments reveal that most of the sands are tinted a yellow-red color indicating the presence of iron oxide coatings (Puckett and Cowdery, 2002). Similarly, the UND denitrification team observed fine grained reddish precipitation of Fe(III)-oxyhydroxide at one of the springs located in the Akeley aquifer, which indicates the presence of dissolved Fe(II) in the groundwater.

Based on the hypothesis made during the beginning of the research, an alternative scenario followed during my research was an approach that takes into consideration all the common electron donors. However, the significance of Fe(II)-supported denitrification process was given special emphasis in the project because it has been less understood in our region. Geochemical modeling using PHREEQC was employed to resolve the complication between the two precipitating denitrification reaction products (inorganic carbon and Fe(III)-oxyhydroxides).

Iron Geochemistry and Denitrification

Iron is the most abundant metal and is believed to be the tenth most abundant element in the universe (Wikipedia online Encyclopedia: <http://en.wikipedia.org/wiki/Iron>). It is also the fourth most abundant redox element in the earth's crust (e.g. Fe in Earth's crust is ~ 5.09 mass % and in sedimentary environments ~ 3.09 mass %) and the average Fe(III)/Fe(II) ratio is ~ 1.35 (Shelobolina et al. 2003 and references therein). Redox diagrams show that in the normal pH range (5 - 8) of natural waters dissolved iron is dominantly as Fe(II), while Fe(III) is insoluble (Appelo and Postma, 1996).

The main sources of ferrous iron in groundwater are the dissolution of Fe(II)-bearing minerals and the microbial reduction of Fe(III)-oxyhydroxides present in the sediments (Appelo and Postma, 1996). Aquifer Fe(II)-bearing minerals are magnetite (Fe_3O_4), ilmenite (FeTiO_3), pyrite (FeS_2), mackinawite (FeS), siderite (FeCO_3), and Fe(II)-bearing silicate minerals, like amphibole (grunerite $\text{Fe}_7\text{Si}_8\text{O}_{22}(\text{OH})_2$), pyroxene (ferrosilite $\text{FeMgSi}_2\text{O}_6$), biotite ($\text{KMg}_{2.5}\text{Fe}^{2+}_{0.5}\text{AlSi}_3\text{O}_{10}(\text{OH})_{1.75}\text{F}_{0.25}$), olivine ($(\text{Mg,Fe})_2\text{SiO}_4$), glauconite ($\text{K}_{0.6}\text{Na}_{0.05}\text{Fe}^{3+}_{1.3}\text{Mg}_{0.4}\text{Fe}^{2+}_{0.2}\text{Al}_{0.3}\text{Si}_{3.8}\text{O}_{10}(\text{OH})_2$), chlorite (chamosite/clinochlore $(\text{Fe,Mg})_5\text{Al}(\text{Si}_3\text{Al})\text{O}_{10}(\text{OH})_8$), etc. (Appelo and Postma, 1996).

Most of these minerals, under normal circumstances, have complex dissolution processes that are controlled by the redox state of the system and microorganisms (Kehew, 2001). For example, the release of Fe(II) is faster in anoxic conditions than under oxic environments (Appelo and Postma, 1996). Microorganisms catalyze the release of Fe(II) for their own metabolic needs and gain energy from the Fe-cycle through both Fe(III) reduction to Fe(II) and oxidation of the latter to Fe(III) (Shelobolina et al. 2003).

Information is scarce regarding the redox reactions between nitrates and dissolved ferrous iron and even fewer studies have been able to show the significance of solid phase ferrous iron. Postma (1990) showed how Fe(II)-rich pyroxenes and amphiboles react (at an approximate rate of $4.0\text{E}-05 \text{ NO}_3^- \text{ mol/L/year}$ at $T \sim 25^\circ \text{ C}$) chemically with nitrate in the presence of some catalysts. Lately, less expensive abiotic chemical treatment of nitrate with fine grained Fe(0) has gained popularity (Devlin et al., 2000); however, it still requires some engineering work and obviously is not recommended for aquifer-scale remediation processes.

Ernstsen (1996) studied the reduction of nitrate by Fe(II)-rich chlorite in one of the Danish aquifers. He showed how the reduction of nitrates correlated with the abundance of Fe(II) minerals, while the amount of the total iron remained nearly constant. The study area is a confined aquifer of 14 Ka to 15 Ka years of age and was deposited by glacial processes. The aquifer is also overlaid by intensive agricultural activities. Ernstsen (1996) also recommended further study on the role of microorganisms.

Many researchers have shown evidently the role of microorganisms in aquifer redox reactions (Straub et al. 1996; Benz et al. 1998; Sobolev and Roden, 2002). Rogers and Bennett (2004) explained that microorganisms exist at depths exceeding 3 km and at

temperatures greater than 100 °C. Various earlier studies also show that denitrifying bacteria represent a large fraction of all bacteria present in sediments (Lovley and Coates, 2000; Hauck et al. 2001 and references therein; Straub et al. 2001). Hauck et al. (2001), from a lake sediment study, also explained that ferrous-iron-oxidizing denitrifying bacteria make up about 58% of the total denitrifying bacteria. Weber et al. (2001) found significant NO_3^- reduction by microbial mediated Fe(II) rich solid phases. In contrast, insignificant denitrification reactions were observed in the abiotic cultures treated with heat. Liermann et al. (2000) have also shown that biotic dissolution of hornblende is significantly higher than that of the abiotic. A study on the anoxic layer of urban Upper Mystic Lake (Massachusetts, USA) also demonstrated that nitrate controls the redox state of iron by oxidizing Fe(II) to Fe(III) (Senn and Hemond, 2002). Weber et al. (2001) reached the conclusion that microbial activity has the potential to facilitate the reduction of nitrates by ferrous iron in sedimentary environments. Microorganisms preferentially colonize selected aquifer minerals for their nutritional benefits and catalyze the dissolution of silicates containing iron and phosphorus (Rogers and Bennett, 2004; and the references therein). Iron is needed by most organisms for their enzyme functions and respiratory systems (Kalinowski et al. 2000). Microorganisms facilitate silicate dissolution by producing organic acids (lowering pH); while secretion of an organic ligand siderophores (chelating agents secreted by bacteria and fungi) initiate redox reactions (Rogers and Bennett, 2004).

A regional study performed close to three of the ISM research sites (Akeley, Perham-M and Perham-W) in west-central Minnesota glacial outwash aquifers demonstrated that denitrification is one of the major processes that removed considerable amounts of NO_3^- (Puckett and Cowdery, 2002). The authors, however, recommended more comprehensive investigation on the spatial extent of the role of the denitrification reaction as a bioremediation process. Böhlke et al. (2002) explained more specifically that Fe(II) phases and pyrite are important electron donors in glacio-fluvial aquifers in central Minnesota. They observed the occurrence of yellowish and reddish Fe(III)-oxyhydroxide coatings in the aquifer sediment samples and indicated that the Fe(II) source minerals are biotite, amphibole, magnetite, and pyroxenes.

Hence, aquifer sediments with high iron contents, reducing conditions and microorganisms capable of reducing Fe(III) to Fe(II) (Fig. 2) will likely support denitrification by Fe(II).

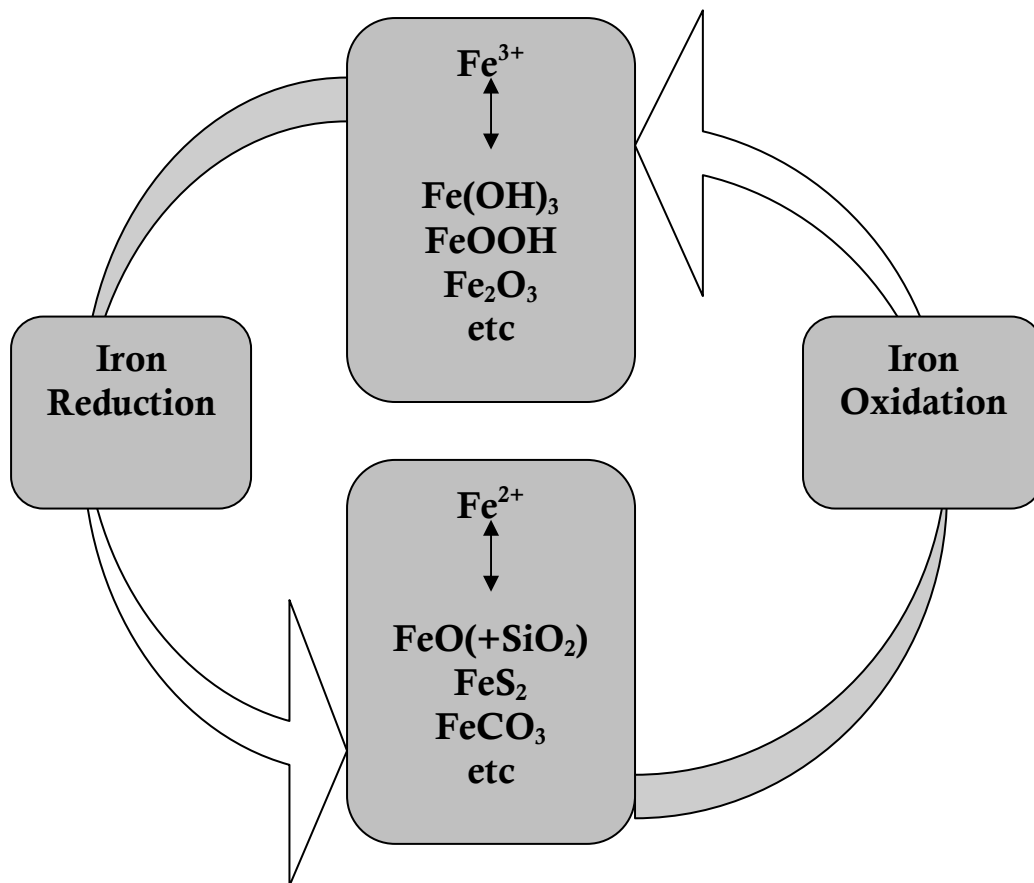


Figure 2. Iron Cycle in Environmental Biogeochemistry (After Schröder et al., 2003).

Analytical Methods and Results

Subsurface sediment cores were collected from below the water table from all sites with a truck-mounted drill rig provided by NDSWC. The samples were taken from the ISMs or next to them. Sediment samples were stored in jars flushed with nitrogen to minimize atmospheric contamination. Some samples were also transported back to UND in a nitrogen-filled glove box. All cores were immediately sectioned, sealed in containers, and stored in a nitrogen-filled glove box as soon as they arrived at UND. The samples were used to analyze mineralogy, texture, organic carbon contents, inorganic sulfide (dominantly pyrite) contents, ferrous iron contents and CECs of the sediments. Organic carbon was determined by a high temperature combustion method (Churcher and Dickout, 1986) and inorganic sulfide was measured by a chromium reduction method (Canfield et al., 1986). Only sediment smaller than gravel was analyzed during the geochemical analyses. For organic carbon analysis, samples were pre-treated with HCl acid ($\text{pH} < 2$) to remove inorganic carbon. The presence of high amounts of inorganic carbon commonly complicates the measurement of organic carbon.

Then the samples were filtered, weighed, and dried in an oven at 104 °C oven for 24 hours so that the net inorganic carbon removed from the sample could be determined. Finally, the measured organic carbon of the acidified samples was corrected to represent the organic carbon content with respect to the total sample.

Texture analysis of the aquifer sediments was done by settling velocities and hydrometer readings (ASTM, 1993). A summary of the results for Akeley, Robinson, and Kalrsruhe-S are given in Figure 3.

CEC of sediments from all nine ISM sites, plus three duplicate samples, were analyzed at the Soil Laboratory, North Dakota State University, Fargo. However, laboratory values for CEC are commonly overestimated (Barton and Karathanasis, 1997; Amini et al., 2005). Based on in situ estimates of CEC with a geochemical modeling (Parkhurst and Appelo, 1999), the lab values were found to be high and were not used. Because of the importance of Fe(II) to this research a separate section on ferrous iron analytical methods and results follows.

**Texture Analysis of North Dakota and Minnesota Aquifer
Sediment Samples**

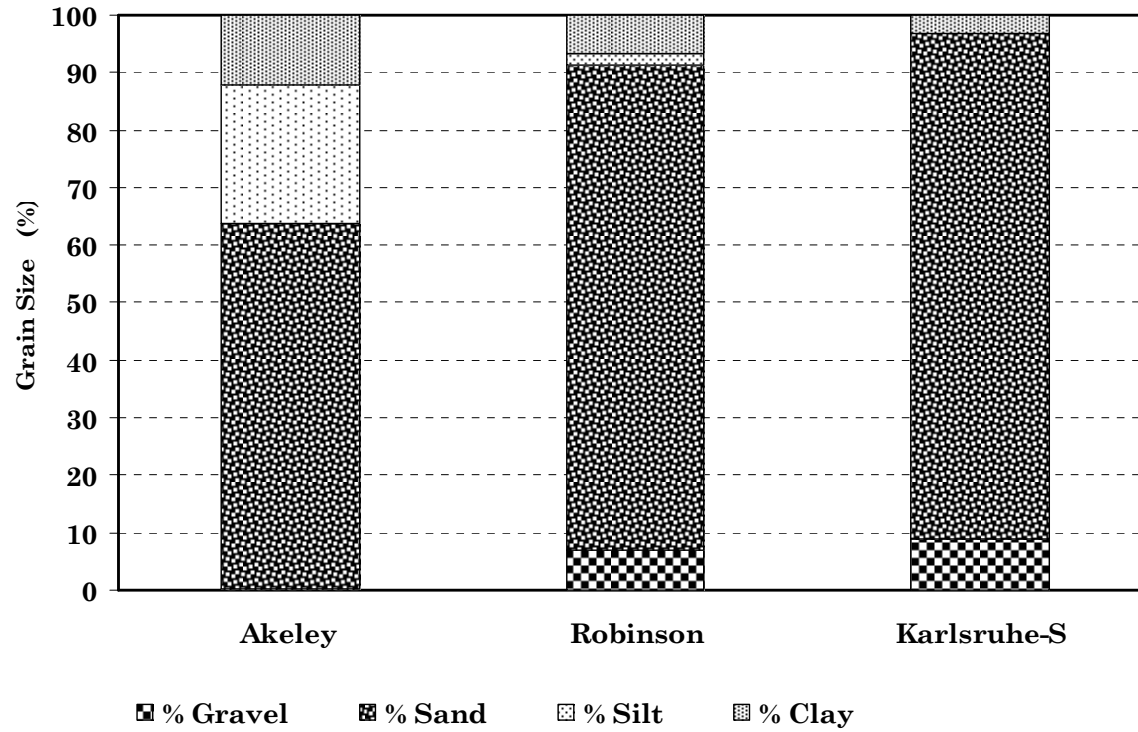


Figure 3. Texture Analyses of Aquifer Sediments for Akeley (MN), Robinson (ND) and Karlsruhe-S (ND).

Ferrous Iron Analytical Methods and Results

During the beginning of the project, I was hoping to find simple Fe(II)-bearing solid phases, such as siderite. However, it became clear that the predominant Fe(II)-bearing minerals at our ISM sites are primary and secondary silicate minerals of complex solid solutions. Silicate minerals not only have complex dissolution stoichiometry, their thermodynamic data are also scarce and variable (Palandri and Kharaka, 2004). Furthermore, silicate minerals can be dissolved through congruent, incongruent, and oxidative dissolution reactions, usually at a very low rate unless catalyzed by microorganisms (Kehew, 2001). For example, the common iron-bearing minerals determined at our research sites have comparable dissolution rates (mole m^2/s , pH near neutral, 25 °C): biotite $\log K \sim -12.55$, clinocllore $\log K \sim -12.52$, and amphibole $\log K \sim -10.30$ (Palandri and Kharaka, 2004). Three analytical techniques: wet chemical extraction, x-ray diffraction, and Mössbauer spectroscopic measurements, were used to determine ferrous iron contents and Fe(II)-bearing minerals present. Combining the results of the three methods reduces the ambiguity of identifying the Fe(II)-bearing minerals and the amount of Fe(II) present in them.

Chemical Extraction

Ferrous iron in various forms was measured through wet chemical extraction by adopting methods used by Heron et al., (1994), Linge (1996), and Kennedy et al. (1999). The three different Fe(II) forms were the “adsorbed fraction” (extracted with 1 M $CaCl_2$), the “amorphous Fe(II) fraction” (extracted with 0.5 M HCl) and “total ferrous iron” (extracted with hot 5 M HCl) (Heron et al., 1994; Linge, 1996, Kennedy et al., 1999). The adsorbed fraction appeared to be insignificant and is not discussed further. Amorphous ferrous iron is the most reactive Fe(II) iron fraction in aquifer sediments (Heron et al., 1994). Wet chemical extractions were completed at UND’s Environmental Analytical Research Laboratory (EARL). One of the challenges of analyzing ferrous iron was keeping the solution in a reduced state during the analytical process. A nitrogen atmosphere had to be used for all the analytical procedures, starting from weighing samples through digestion. Then the analyte was measured using a DR/2010 Spectrophotometer. Incomplete dissolution of minerals is possible (Lalonde et al., 1998). The results of the analyses for Akeley, Robinson, and Karlsruhe-S are given in Table 1 and Figure 4.

X-Ray Diffraction

X-ray diffraction (XRD) analyses provide important semi-quantitative information of well-crystallized dominant minerals. Poorly crystallized minerals are usually overlooked (Pope et al., 2002). XRD measurements were used to determine the bulk mineralogy of sediment samples and, thus, sediments smaller than gravels was used in the analyses. Commonly, detection limits of XRD for minerals ranges from 1% to 3% (by weight) depending on background noise, peak resolution of the diffractogram pattern, and sample preparation (Zachara et al., 2004). The X’Pert advanced XRD machine (Department of Physics, UND) has copper targets (anode). Nine samples, one from each ISM site, plus one pre-sieved sample ($< 63 \mu m$) from Larimore and one siderite standard were

Results of Wet Chemical Extractions

Table 1. Geochemical Analyses of Organic Carbon, Inorganic sulfide* and Ferrous Iron for Akeley (MN), Robinson (ND) and Karlsruhe-S (ND).

Study site	Depth ft	% In organic Sulfide* (dominantly pyrite)	% Organic Carbon	% Fe (II) _a (Amorphous)	% Fe(II) _t (Total)	
Akeley (MN)	15 - 17	0.007 (4) ± 0.001	0.024 (5) ± 0.008	0.113	0.205	Fe(II) _a duplicate = 0.105
Robinson (ND)	23.5	0.024 (3) ± 0.016	0.077 (2) ± 0.009	0.089	0.172	Fe(II) _a duplicate = 0.124
Karlsruhe-S (ND)	16 - 21	0.194 (4) ± 0.074	0.017 (3) ± 0.007	0.227	0.490	
Standards						
Pyrite		52.42 (2) ± 0.863		0.03	0.02	
Siderite				47.47	48.16	
CaCO ₃			12.00			
C ₆ H ₁₂ O ₆			40.00			

Remarks

Percentages (%) are weight % per sample.

The numbers inside brackets indicate the number of analyses. Standard deviations (±) are also given.

Pyrite (FeS₂*) is also dominant form of sulfides and is used interchangeably with inorganic sulfide.

Chromium reduction methods of analyses for Sulfide shows 98% recovery while Fe(II)-silicate analytical method is proved to be ineffective for Fe(II)-in pyrite.

CaCO₃ was used for plotting the calibration curve for the results of inorganic carbon ($r^2 \sim 0.99-1.00$). C₆H₁₂O₆ was also used for plotting the calibration curve for the results of total carbon ($r^2 \sim 0.99-1.00$).

I am using the last analyses for Fe(II) results because my methodology improved with experience. Furthermore, I did not use the standard deviation because unlike for sulfide and organic carbon, I had to use wet samples and they are usually vulnerable to uncertainties associated with the computation of moisture contents.

Pure Pyrite has 53.45% sulfide.

Pure Siderite has 48.20% Fe(II).

Pure CaCO₃ has 12.00% carbon.

Pure C₆H₁₂O₆ has 40.00% carbon.

Results of Chemical Extraction: Electron Donors

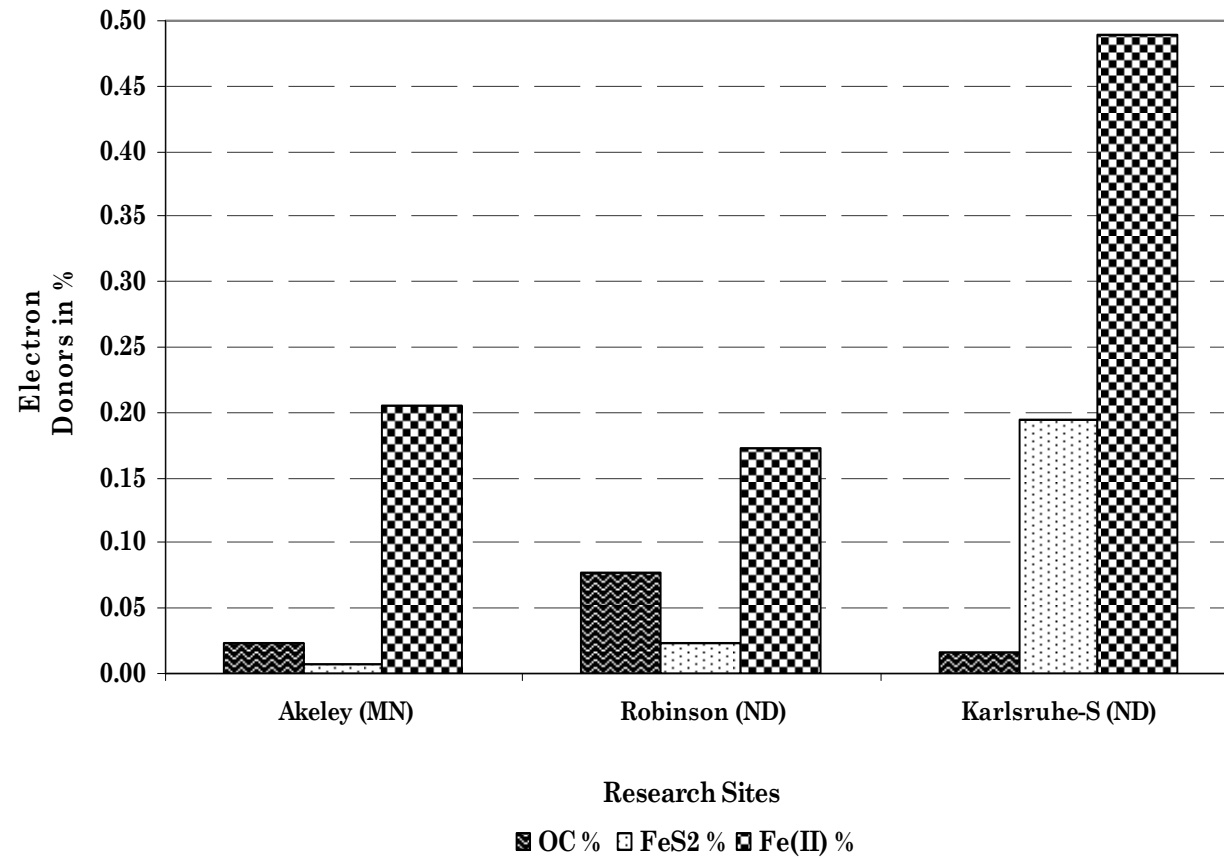


Figure 4. Results of Wet Chemical Extraction (Ferrous Iron), High Temperature Combustion Method (Organic Carbon Analyzer) and Chromium Reduction Method (Sulfide) for Akeley (MN), Robinson (ND) and Karlsruhe-S (ND) (% by weight per each sample).

analyzed. XRD scans were matched, based on the so-called "figure-of-merit" with a standard mineral database [ICDD PDF2 (2002)] loaded in the X'Pert machine. The results of the three research sites, Akeley, Karlsruhe-S, and Robinson are given in Figures 5-7, respectively.

As expected the dominant minerals, quartz, plagioclase feldspar, alkali feldspar, calcite and dolomite are common to all the samples. However, the occurrence and abundance of the most important Fe(II) bearing minerals, chlorite (clinochlore), amphibole (hornblende), pyrite, and biotite and/or muscovite (because of the overlapping peaks) vary from place to place. The small peaks, such as for pyrite and chlorite (clinochlore), in XRD measurements apparently cannot be used to quantify the abundance of minerals, likely because of background noise. In general, however, amphibole has larger peaks compared to those for pyrite and clinochlore. Amphibole (as hornblende) has relatively larger peaks in Akeley and Karlsruhe-S, and moderate peaks in Robinson. As will be explained in the next subsection, those observations are consistent with the results obtained from the measurements of the wet chemical extraction and Mössbauer spectroscopy.

The pre-sieved (< 63 µm), or concentrated sample, had no detectable clinochlore, but displayed a relatively larger pyrite peak; the amphibole peak was the largest of all samples analyzed in this project. This implies that crystalline amphibole is relatively abundant, whereas crystalline clinochlore has low abundance, in the clay fraction of the Elk Valley sample, which is consistent with the stability of primary silicate minerals. The background noise around clinochlore is relatively high but no significant peak was observed; it may imply the clinochlore is a secondary mineral and it is poorly crystallized. Primary minerals such as amphibole are less stable compared to clay chlorite (clinochlore) and are therefore more abundant in the small grain sizes.

Table 2. XRD Detection of the Major Minerals for Akeley (MN), Robinson (ND) and Karlsruhe-S (ND)

Mineral Phases	Akeley	Karlsruhe-S	Robinson	Remark
Quartz	+	+	+	
Dolomite	+	+	+	
Calcite	+	+	+	Plagioclase feldspar
Albite/Anorthite	+	+	+	
Microcline/Anorthoclase	+	+	+	Alkali feldspar
Amphibole/Hornblende	+	+	+	
Muscovite/ Biotite	+	+	+	
Clinochlore	+	+	+	Secondary chlorite
Pyrite	+	+	+	

+ Symbolizes the presence of a mineral in the sediment sample.

XRD Scan of Aquifer Sediment Samples from Akeley Research Site, Minnesota.

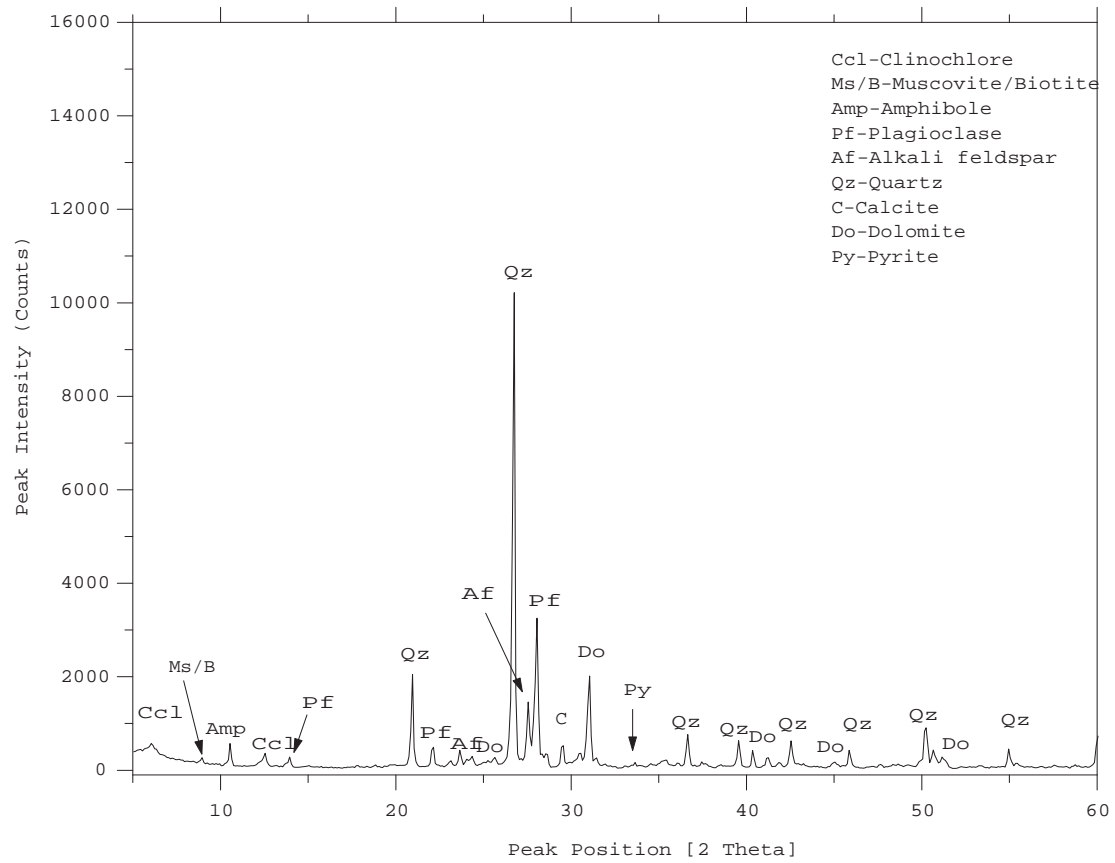


Figure 5. XRD Scan of Aquifer Sediment Sample from Akeley, MN.

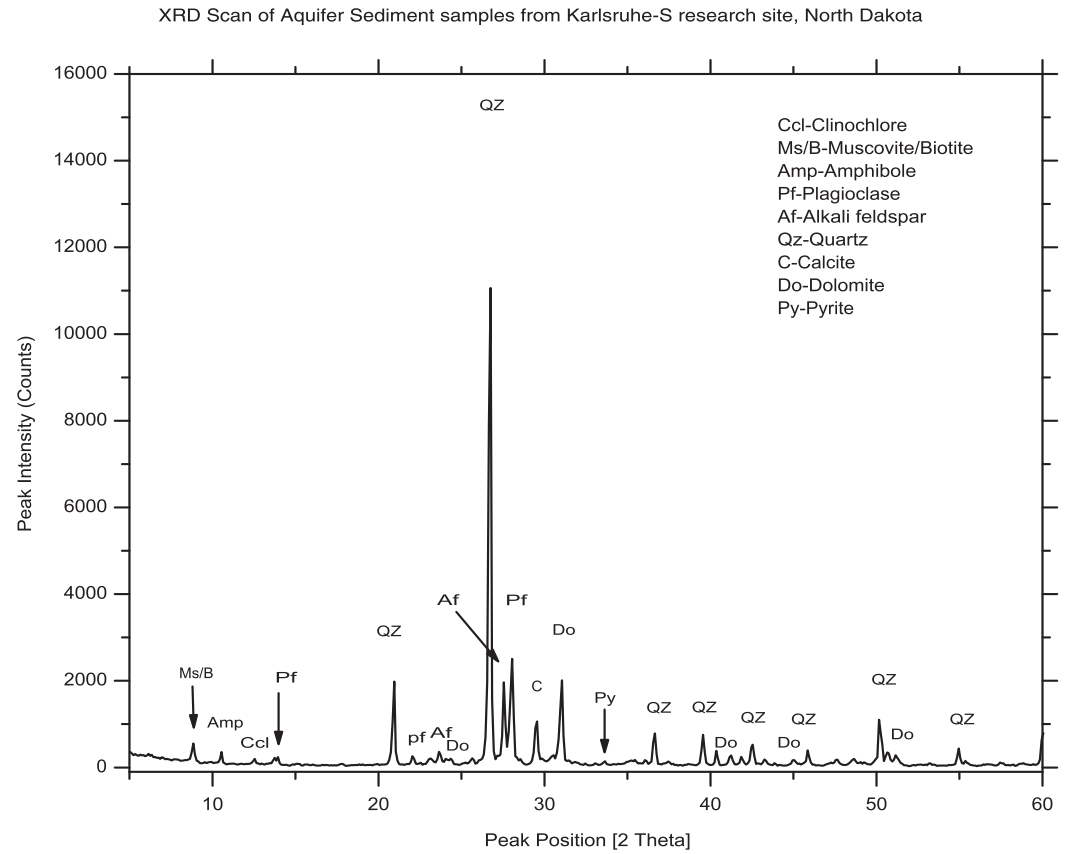


Figure 6. XRD Scan of Aquifer Sediment Sample from Karlsruhe-S, ND.

XRD Scan of Aquifer Sediment Samples from the Robinson Research Site, North Dakota.

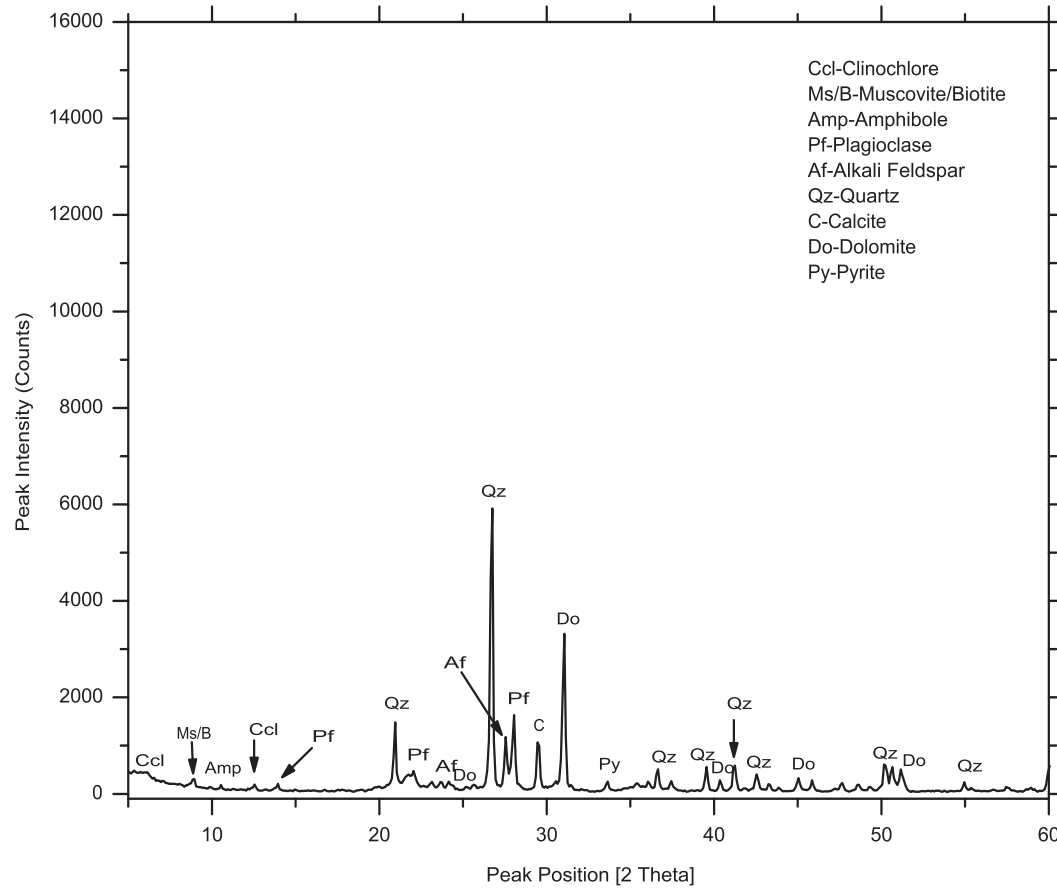


Figure 7. XRD Scan of Aquifer Sediment Sample from Robinson, ND.

Mössbauer Spectroscopy

Mössbauer spectroscopy is an ideal instrument for the analyses of iron-bearing minerals (McCammon, 1995). Since the surrounding electronic, magnetic and chemical environment influences the nucleus (McCammon, 1995), the hyperfine changes (not accessible to direct observation) in the nuclear energy levels can be observed spectroscopically to yield qualitative information about types of Fe(II)-bearing minerals and quantitative information about ferrous/ferric ratios. Isomer shift, quadrupole splitting and magnetic hyperfine interactions are three important Mössbauer parameters. These are resulted from the perturbation of the resonance effect (resonance of emission and absorption lines) due to the difference, which is usually the case when studying iron-bearing minerals, between the absorber and the source, ^{57}Co embedded in rhenium (Dyar and Schaefer, 2004). The difference between the transition energies between the absorber and source is called the isomer shift (δ) (Figure 8) and is given by the difference between the position of the baricenter of the resonance signal and zero Doppler velocity (McCammon, 1995). Iron species have different nuclear spin numbers (S) and $S = 2$ is the most common type of Fe(II) (M. Kanishka, personal communication). Mössbauer spectroscopy is used for measuring ferrous/ferric iron ratios, because Fe(II) has an electronic configuration of $(3d)^6$ while that of Fe(III) is $(3d)^5$. Ferrous ions have less s-electrons at the nucleus due to the greater screening of the d-electrons. Thus, ferrous ions have larger isomer shifts than ferric ions (McCammon, 1995; Dyar and Schaefer, 2004). Quadrupole splitting (ΔE_Q) is the distance between the two centroids of the two main peaks. Magnetic hyperfine interactions are observed for magnetic iron minerals. The Mössbauer Effect Data Center has categorized 400 minerals, based on their isomer shift, quadrupole splitting and magnetic hyperfine interactions, into six major groups (McCammon, 1995). When employing such a large database, there is always an associated problem of uniqueness. Hence, in addition to Mössbauer measurements, other approaches had to be combined to identify the minerals of interest with greater confidence.

Table 3. Mössbauer Spectroscopy Measurements of Aquifer Sediments for Akeley (MN), Robinson (ND) and Karlsruhe-S (Department of Physics and Atmospheric Science Dalhousie University Halifax, Nova Scotia Canada)

Sample	Depth (ft)	Fe(II) %	Fe(III) %
Akeley	17 ft	58	42
Larimore	17.5 ft	21.2	78.8
Karlsruhe-S	16-18 ft	50	50
Robinson	24.5 ft	31	69

Table 4. Replicate Mössbauer Spectroscopy Measurements of Aquifer Sediments for Akeley (MN), Robinson (ND) and Karlsruhe-S (Colorado School of Mines)

Sample	Depth (ft)	Fe(II) %	Fe(III) %
Akeley	17 ft	51	49
Larimore	17.5 ft	26	74
Karlsruhe-S	16-18 ft	65	35

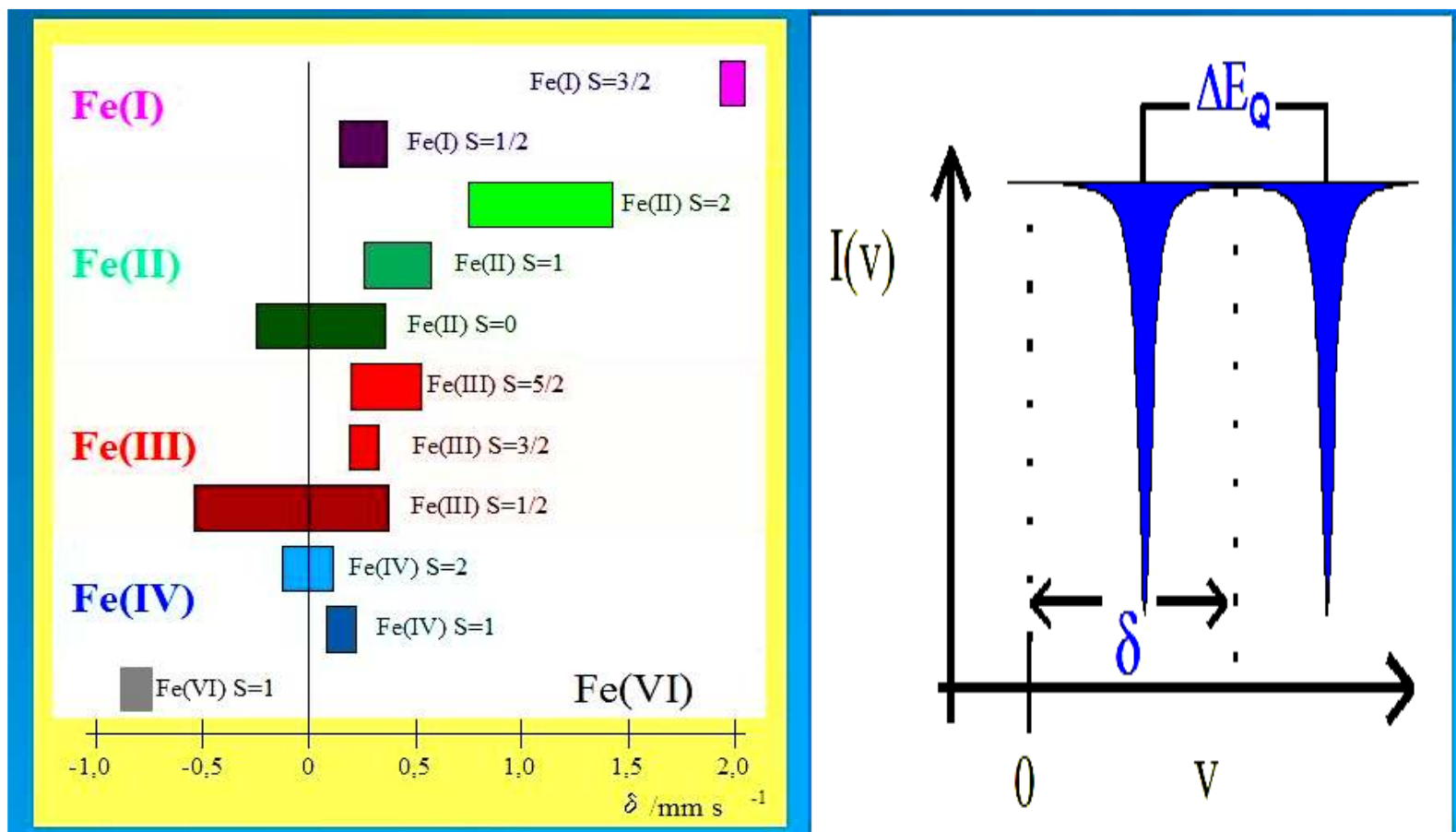


Figure 8. Ranges of Isomer Shifts (δ) for Iron Compounds of Different Oxidation and Spin States and how Isomer Shift and Quadrupole Splitting (ΔE_Q) are Measured from the Mossbauer Spectrum (Modified from Gülich et al. World Wide Web on Mossbauer Spectroscopy)

The difference between the results of Halifax and Colorado Mössbauer spectroscopy measurements may be a result of a weak source for the latter (D. Williams, personal communication to S. Korom). Mössbauer spectroscopy measurements were done in two different places, Dalhousie University (Canada) and Colorado School of Mines. Table 3 and 4 show that ferrous iron occurrence is relatively high in Akeley (Fig. 9) and Karlsruhe-S sites (Fig. 10), moderate in Robinson (Fig. 11). This observation agrees well with the occurrence of amphibole in these sites as detected by XRD. The two Fe(II) hosting minerals determined in the samples are amphibole (primary silicate mineral) and clinocllore (secondary silicate mineral). Therefore, amphibole (grunerite in PHREEQC database) was used as a representative Fe(II)-mineral during redox modeling, which was explained in detail in the next chapter. Besides, lab experiments (at a temperature of 25° C and pH 7) show that amphibole dissolves at a higher rate relative to the rate of dissolution of that of the clinocllore and biotite (Palandri and Kharaka, 2004).

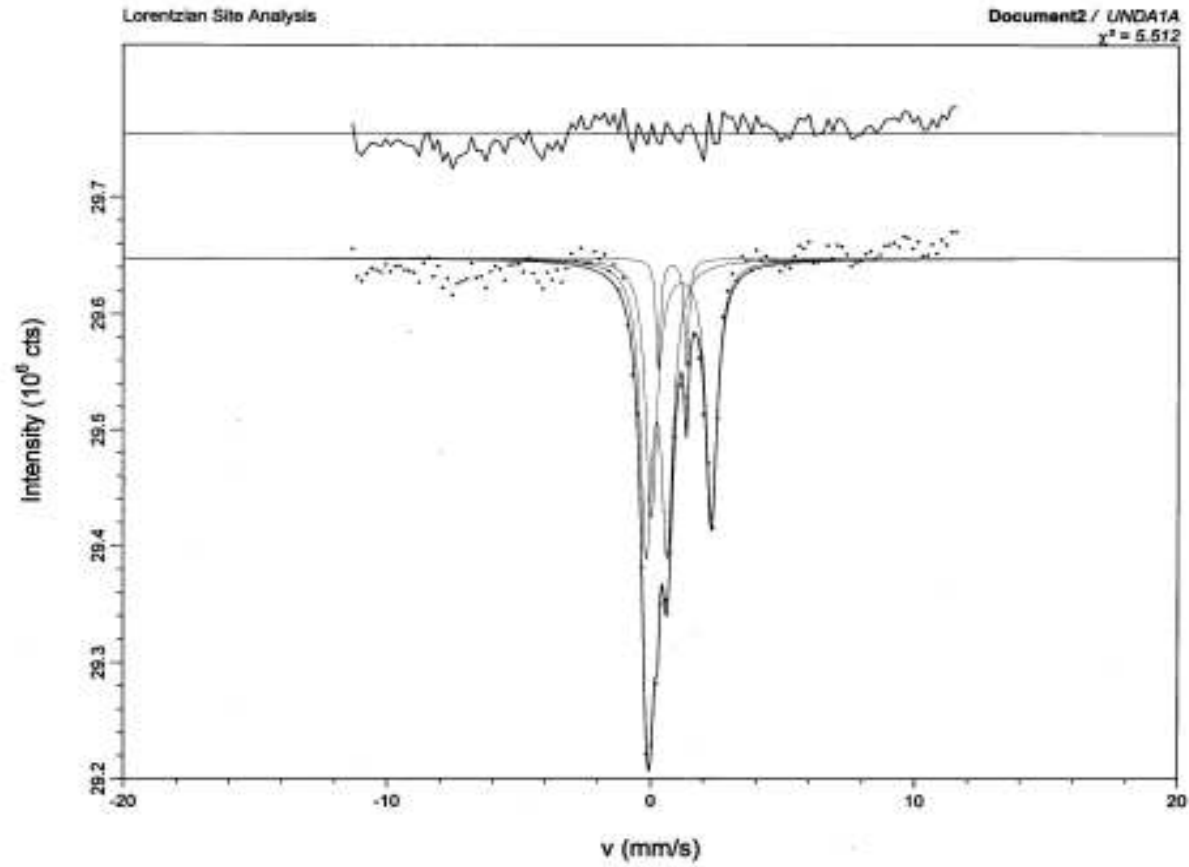


Figure 9. Mössbauer Spectroscopy Measurements of Aquifer Sediment Sample for Akeley, MN (Colorado School of Mines)

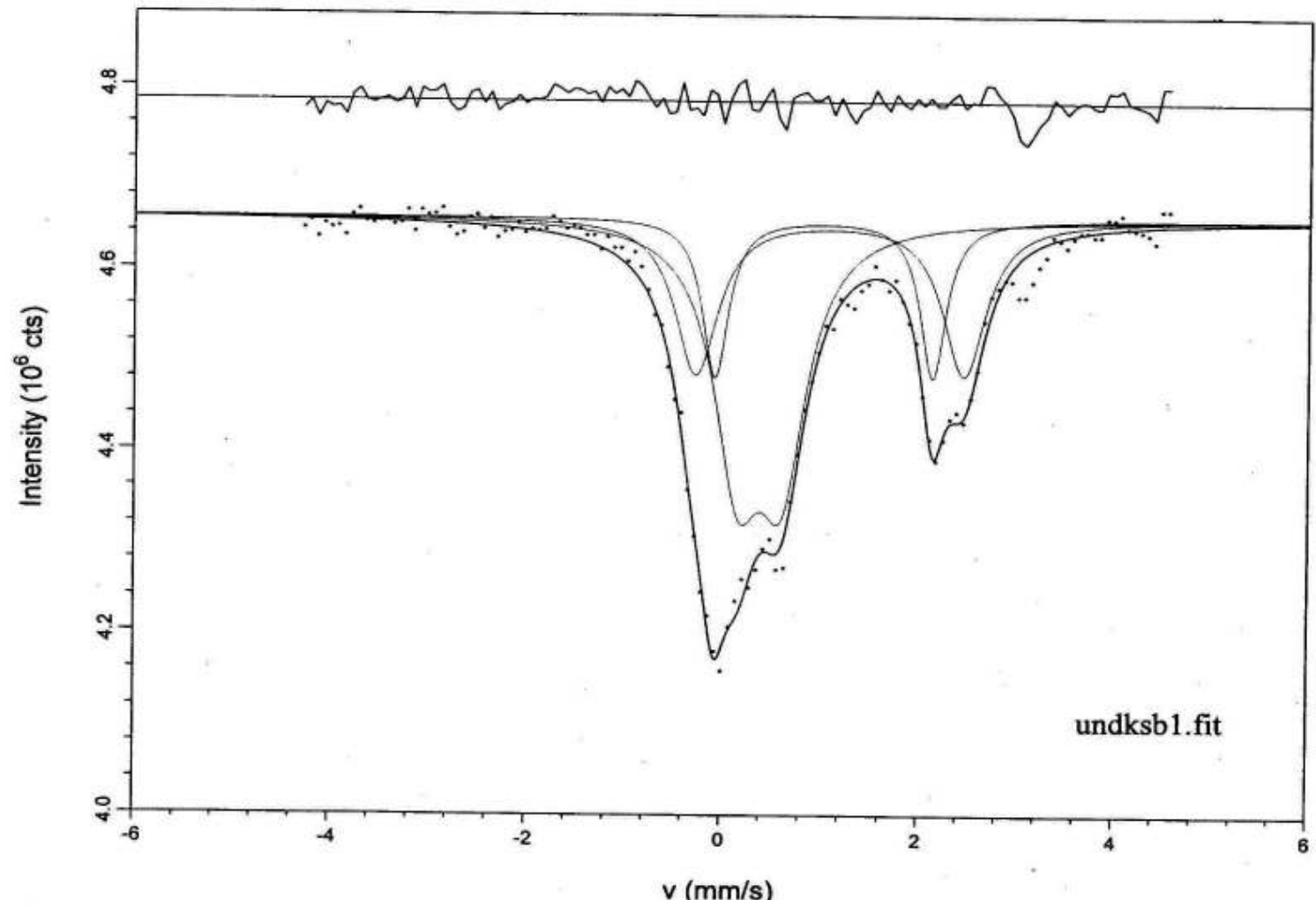


Figure 10. Mössbauer Spectroscopy Measurements of Aquifer Sediment Sample for Karlsruhe-S (ND) (Dalhousie University Halifax).

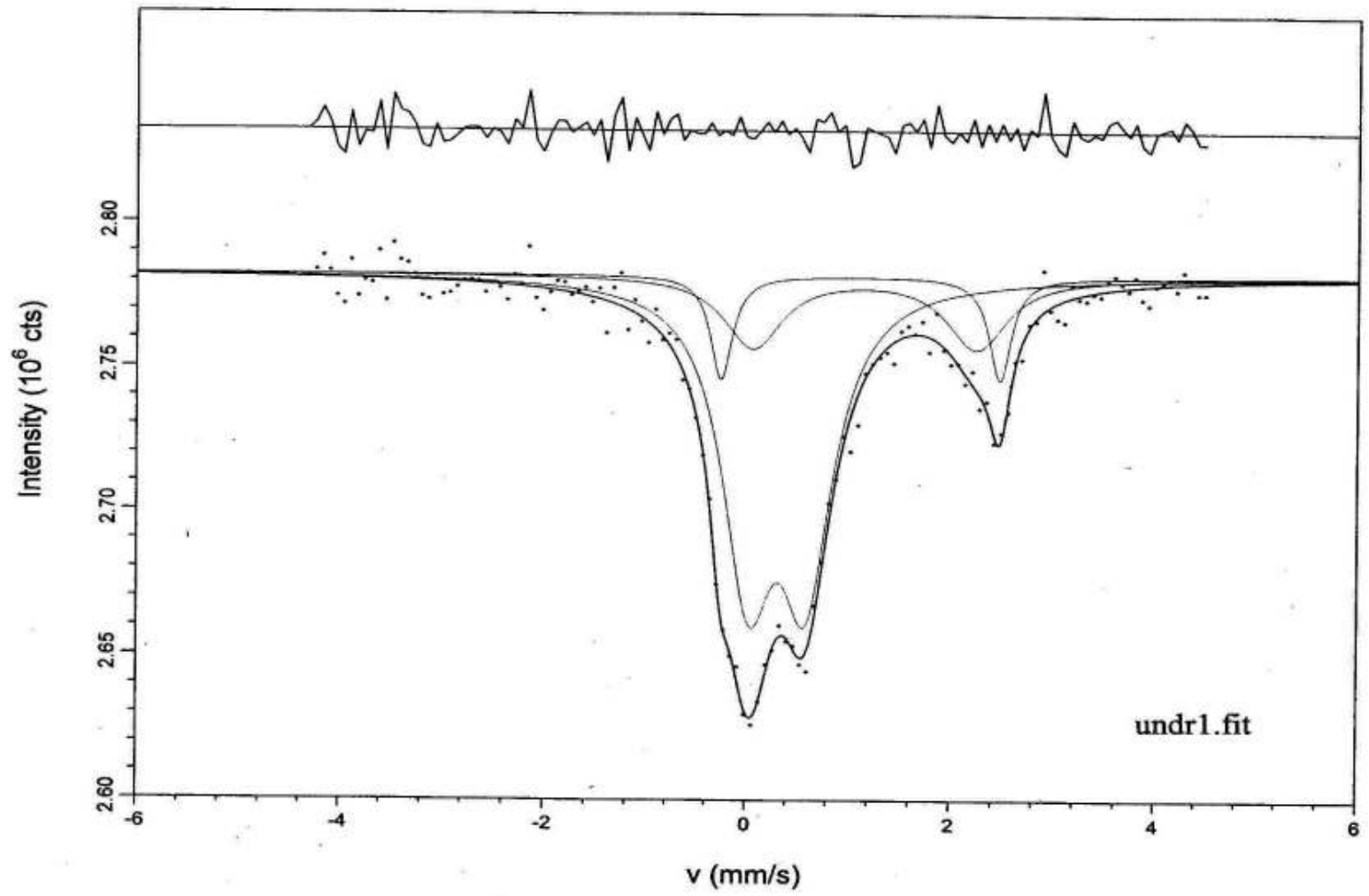


Figure 11. Mössbauer Spectroscopy Measurements of Aquifer Sediment Sample for Robinson (ND) (Dalhousie University Halifax).

Geochemical Modeling Methods

Zhu and Anderson (2002, pp. 18) gave a definition of a model as follows: “A model is an abstract object, described by a set of mathematical expressions (including data of various kinds) thought to represent natural processes in a particular system. The ‘output data’, or the results of the model calculations, generally are quantities, which are at least partially observable or experimentally verifiable. In this sense the model is capable of prediction.” A model, as a simplified version of a natural system, should keep the balance between realism and practicality. Geochemical modeling aids our understanding of the major mineral phase-water reactions that control the geochemistry of the ISMs.

PHREEQC is one of the advanced geochemical models that simulates based on the principles of thermodynamic equilibrium (Parkhurst and Appelo, 1999). The acronym PHREEQC stands for the most important parameters of the model; namely PH (pH), RE (redox), EQ (equilibrium), C (programming language) (Parkhurst and Appelo, 1999). It may be used to address the two major types of geochemical problems: forward and inverse (Parkhurst and Appelo, 1999). I used PHREEQC to mimic the in situ geochemical processes with a particular emphasis on the denitrification reactions that occurred in the ISMs by the major electron donors, namely organic carbon, sulfides (as pyrite) and Fe(II). During the modeling work more focus was given to the last type of electron donor. Strictly speaking, equilibrium geochemical modeling (PHREEQC) may not explain the complex natural aquifer denitrification reactions fully, because it requires consideration of the role of bacteria and kinetic principles (Appelo and Postma, 1996). However, in practice it is customary to take the role of microorganisms and kinetics intuitively. Usually, simulating well-constrained equilibrium-based geochemical modeling provides satisfactory results (Postma et al., 1991). The databases, Pheerq.dat, along with the others included in PHREEQC were used.

Conceptualization of a geochemical model is the first critical step in developing a model; it includes defining the approach to the geochemical problem at hand, initial solution, mass transfer, and nature of equilibrium that occurs over the course of the reaction processes (Bethke, 1996). Forward modeling was used here to study the extent of disequilibrium, resulting from the injection of nitrate to the ISMs, and the denitrification potential of the ISM sites that strives to bring back the original pre-injection geochemical environment of the ISMs. Moreover, other related chemical and physical processes were also considered and field and lab data collected from both C-ISM and N-ISM were used to build the following modeling structure (Fig. 12).

Forward Reaction Model

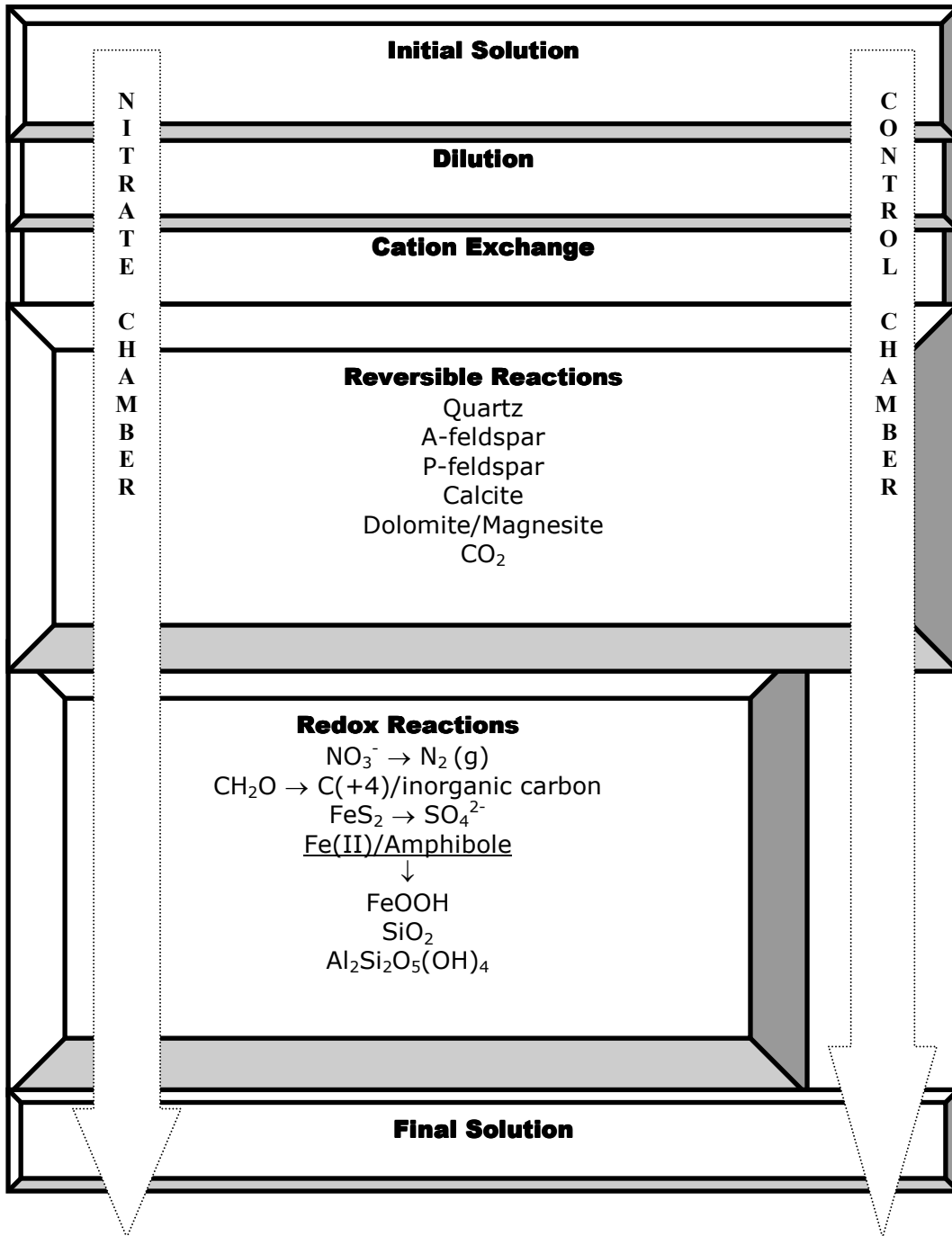


Figure 12. Forward Reaction Modeling Conceptual Representation for Control and Nitrate Chambers.

Forward Reaction Modeling

Forward modeling is constrained by equilibrium thermodynamics; the unknown variables are determined by solving the mass action equations (Parkhurst and Appelo, 1999). It was employed here to understand the evolution of the initial ISM water in response to mixing and geochemical reactions. As illustrated by Figure 12, the major geochemical reactions believed to take place within the ISMs are ion exchange, reversible reactions (dissolution and/or precipitation of dominant minerals), and redox reactions.

Modeling Input data: Initial Solution

Commonly, groundwater geochemistry is controlled by eight major ionic species (Na^+ , K^+ , Ca^{2+} , Mg^{2+} , Cl^- , SO_4^{2-} , HCO_3^- and NO_3^- representing about 95% of all the ions) (Tuccillo et al. 1999; Tesoriero et al., 2000). In addition, for this research, I also considered Mn^{2+} , Fe^{2+} , Si^{4+} (as SiO_2), NH_4^+ , Al^{3+} , F^- , and Br^- , field measured pH, a temperature of 10 °C, and the default value for pe (redox state of pe = 4) to build the initial solution (Solution 0) that served as the input data for the forward modeling. The data were obtained from the analyses of the first sample collected after amendment. For convenience mg/L were converted to mmoles/L. SiO_2 and Al^{3+} values for the Minnesota research sites and Mn^{2+} , Fe^{2+} , and NH_4^+ for some of the North Dakota research sites were either below detection or were not measured. Ruhl (1987) reported water quality data for glacial-drift aquifers in Minnesota and the median value for SiO_2 , as computed from 452 observations, was 19 mg/L (0.32 mmol/L). Therefore, I used that median value for silica (SiO_2) and the detection limit value of 0.00185 mmol/L for Al^{3+} for the MN sites. The missing data (Mn^{2+} , Fe^{2+} , and NH_4^+) for the North Dakota ISM sites were also replaced by their detection values (Appendix C). These values were used to compute the saturation indices of minerals that are relevant to the study. The evolution of each Solution 0 towards the desired solution was tracked by comparing it with the target solutions obtained from field samples. Three target solutions from each site (solutions of ~ 1/3, ~ 2/3 and 3/3 of the total time for the tracer test) were selected, as explained in detail in the next chapter, to verify modeling results.

Dilution

Corrections were made for the ions associated with the tracer Br^- (as Na or K salt) and NO_3^- of the initial solution, based on the dilution observed in the Br^- . Since the background concentrations of Na/K for all the sites but Robinson were < 20 mg/L, it was assumed inconsequential during the dilution of the amended water. No corrections were needed for the rest of the cations and anions because the tracer was assumed not to affect them directly. Accordingly, for each time step, the initial solution included measured values for Br^- ; the values of Na^+/K^+ and NO_3^- from solution 0 for each ISM were corrected by the bromide-dilution ratio.

Cation Exchange Processes

Measurements of the anions (Br^- and NO_3^-) and cations (Ca^{2+} , Mg^{2+} , Na^+ , and K^+) of interest were made of the water before and after amendment, but prior to the injection of the tracer salt. Initially, the cations were assumed to be in equilibrium with the sorbent and solution, but the introduction of Na^+/K^+ with the tracer Br^- to the ISMs caused desorption of other cations (mainly Ca^{2+} and Mg^{2+}) to achieve a new equilibrium status (Kehew, 2001). Anion exchange was excluded from the modeling because most aquifer mineral surfaces are negatively charged in the pH range (pH~ 6.5 – 8.5) of the groundwater environments studied herein (Kehew, 2001). Therefore, Br^- was assumed to be conservative. Decreases in the cation associated with the Br^- (either Na^+/K^+) beyond that of the Br^- were attributed to processes unrelated to dilution, mainly cation exchange. As a result, the relative concentrations of Na^+/K^+ in solution were significantly lower than the Br^- . The Akeley (C-ISM and N-ISM) experienced noticeable cation exchange, whereas Robinson (C-ISM and N-ISM) and Karlsruhe-S (N-ISM) nitrate chambers did not.

Cation exchange processes are relatively fast (Appelo and Postma, 1996) and should occur within a few days of the amendment. PHREEQC uses the Gaines-Thomas convention to quantify the amount of cations (in meq/L) desorbed from minerals surfaces (Parkhurst and Appelo, 1999). It requires defining the non-specific cation exchange capacity X^- (mmol/L) under the keyword “EXCHANGE” and it should be linked to the solution in equilibrium with it through the keyword “EQUILIBRATE”.

There are three ways of computation for the non-specific cation exchange capacity of the mineral surfaces. They are conventional laboratory measurements, estimation using empirical formulas, and in situ CEC simulation through modeling. Conventional laboratory CEC measurements overstate the in situ mineral surface reactions. Barton and Karathanasis (1997) discovered, from eight morphologically and physicochemically different pairs of intact and disturbed soils that lab CEC measurements relatively overestimate ion-exchange processes. Empirical formulas are also questionable because aquifer sediments are highly heterogeneous. The third method was used because it reflects the in situ cation exchange processes. Numerous runs through PHREEQC were performed using different values for the exchanger (X^-) until a good match was achieved between the modeled and the measured analytical data. The major cations (Ca^{2+} , Mg^{2+} , Na^+ , and K^+) from the samples collected before and after the injection of the tracer were compared using the least squares method. Once a satisfactory value for the exchanger X^- was found, the same value was used throughout the modeling exercise for that site.

CEC was included for two reasons. Firstly, for some of our sites it influences the cations of the solution significantly. Secondly, determining the approximate amount of Ca^{2+} and Mg^{2+} on the sediment exchanger sites enabled me to estimate the highest amount of inorganic carbon that may subsequently co-precipitate out from the solution with these cations. The latter is important because in some of our sites denitrification by organic carbon and ferrous iron produce reaction products that may precipitate out of solution. Hence, CEC simulation was used to determine the maximum amount of Ca^{2+} and Mg^{2+} in solution and on exchanger sites that could have precipitated with inorganic carbon. For example, using the X^- value of N-ISM of 3.5 mmol determined by Skubinna (2004) through PHREEQC simulations; the net Ca^{2+} and Mg^{2+}

exchanged for K^+ are about 0.501 mmol/l. This in turn can augment the role of organic carbon by about 17% - 24% (for the Time = 589 days with a net nitrate amount of 2.42 mmol/l). As mentioned earlier pyrite accounts for about 48% of nitrate sink (Skubinna, 2004); therefore, it is essential that another electron donor, presumably Fe(II), be involved in order to explain logically the net nitrate lost in the N-ISMs by denitrification reactions.

Reversible Reactions

Next in the modeling sequence are reversible reactions, where the initial solution, after correction for dilution effects and equilibrium with CEC, was allowed to equilibrate with the major minerals of the research sites using the key word "EQUILBRIUM PHASES". This keyword requires values for the saturation indices and amounts of the minerals involved in moles. Default amounts of the mineral and gas phases (partial pressure values) were 10 moles for dissolving and 0 moles for precipitating minerals. PHREEQC modeling provides better saturation indices because it calculates based on the principle of ion-association (inclusion of all complexes of a given ion) and considers the effect of ionic strength on activity coefficients (Parkhurst and Appelo, 1999; Zheng, 2002).

First, the previously selected solutions (solution 0, solutions of 1/3 and 2/3 of the total time, and the final solution) were computed for the equilibrium states (saturation indices) of the minerals of interest based on water samples. A negative saturation index (SI) indicates undersaturation, while positive and zero values indicate oversaturation and equilibrium, respectively. The XRD-determined major minerals of plagioclase feldspar, alkali feldspar, quartz, calcite, and dolomite were used with CO_2 (Table 2). The partial pressures of CO_2 in the ISMs were greater than its atmospheric abundance, which indicates the anaerobic state (causing oxidation of organic carbon) of the ISMs.

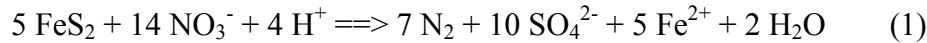
During the simulation of the reversible reactions, the minerals were forced to react until the SI values were attained for all the interacting phases based on the water samples mentioned above. That means the simulated solutions were forced toward the measured values by dissolving or precipitating the major minerals as dictated by the in situ negative and positive SI values, respectively.

The above processes, dilution, cation exchange, and reversible reaction simulations are common for both C-ISMs and N-ISMs. The simulated results for C-ISMs were compared with the target solutions of each time step, whereas the model outputs of the N-ISMs were saved for further simulations involving redox reactions.

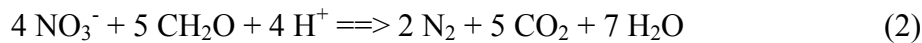
Redox Reactions

The injection of the oxidant nitrate into the relatively reduced water instigates important multiphase aquifer redox reactions that change the fate of the redox-sensitive contaminant NO_3^- (Kehew, 2001). The keyword "REACTION" was used to model redox reactions. It requires the amounts of nitrate reacted with the electron donors. The net amount of nitrate for each time step was computed by determining the nitrate lost since the previous time step and subtracting from it the portion lost due to dilution. Then electron donors were reacted sequentially with the amount

of nitrate lost: first pyrite, then organic carbon, and finally ferrous iron (as amphibole). Complete oxidative dissolution of the reductants, with the help of the catalytic action of microbial organisms, was assumed for all redox reactions. Theoretically, the proportion of the three electron donors could be determined from their respective reaction products measured from the water samples; however, in practice only sulfate from the oxidation of pyrite was measured with confidence. The amount of pyrite reacted for each time step was calculated from the net sulfate increase measured in the aqueous samples since injection according to Equation 1.

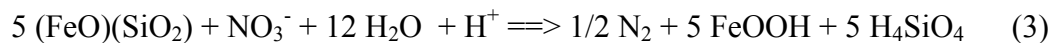


Sulfate minerals, such as gypsum ($\text{CaSO}_4 \cdot 2\text{H}_2\text{O}$), Na-jarosite ($\text{NaFe}_3(\text{SO}_4)_2(\text{OH})_6$) and K-jarosite ($\text{KFe}_3(\text{SO}_4)_2(\text{OH})_6$), were undersaturated during the tracer tests; therefore, all sulfate produced was assumed to remain in solution. The amount of organic carbon that contributed to denitrification was estimated in two ways. It can be estimated directly from the net inorganic carbon increase measured during the entire sampling period (Equation 2).



On the other hand, in some of our research sites it happened that there were no increases of inorganic carbon, even though organic carbon was probably involved, due most probably to precipitation of Ca-Mg- CO_3 (Schlag, 1999; Korom et al., 2005). In the latter case, the inorganic carbon produced and precipitated was estimated by computing the total amount of co-precipitating cations, Ca^{2+} and Mg^{2+} , lost from solution, including the fraction desorbed from mineral surfaces as explained previously in the CEC subtopic. Therefore, using the “REACTION” keyword, organic carbon may also explain the loss of some nitrate not denitrified by pyrite.

By process of elimination, the remaining nitrate sink was attributed to ferrous iron (as amphibole) that presumably resulted into precipitating Fe(III)-oxyhydroxide phases (Equation 3).



Some minor adjustments were made on both organic carbon and Fe(II) amounts based on the modeling output results because the amount of organic carbon computed indirectly provided a range of values and “REACTION” modeling was done initially using the upper limit. When organic carbon and pyrite (sulfide) were supporting the denitrification processes, the reaction products are commonly implicitly understood. Sulfate can be measured from the analysis of the periodically collected aqueous samples, while inorganic carbon can be estimated directly or indirectly. However, oxidative dissolution of Fe(II)-rich primary silicate phases by nitrate gives rise to other secondary solid phases. Secondary silicate minerals (clay minerals) and Fe(III)-minerals are many and variable; nevertheless, for modeling purposes kaolinite, goethite, and silica (SiO_2) were selected. They were put in as equilibrium phases and PHREEQC determined their equilibrium states automatically, all of which were supersaturated.

Finally, modeling output for each time step was saved in a different file for further data analysis, validation, and interpretation.

Geochemical Modeling Results

As explained earlier in the modeling methodology, reaction simulations demonstrated the proportional roles of the common electron donors. The next task focused mainly on validation and interpretation of modeling results. Modeling results are discussed in detail here for Akeley (MN), Robinson (ND) and Karlsruhe-S (ND), while modeling results for the four research sites, Perham-M (MN), Perham-W (MN), Luverne (MN), Larimore (ND) (second tracer test) are not included here.

Modeled vs. Measured Cations and Anions

Control Chambers (C-ISMs)

For Robinson C-ISM solutions of T279, T518 and T777 were chosen as target solutions (Fig. 13). Numbers refer to time in days since the first sample was taken. The relative concentrations of Na^+ and Br^- were roughly proportional, therefore CEC reactions for Robinson C-ISM were assumed to be insignificant. The main process affecting both was dilution with the less concentrated native water. For the Akeley C-ISM the three solutions chosen to verify the modeling work were samples of T100, T230, T490. The relative concentrations of Na^+ and Br^- demonstrated that Na^+ declined more than Br^- , and the CEC was obtained with PHREEQC. Therefore, solution 0 was treated with the non-specific sorption capacity of X- ~ 0.22 moles, as explained earlier. Accordingly, the major cations and anions affected by CEC equilibrium reactions were Na^+ , Ca^{2+} , Mg^{2+} and inorganic carbon (HCO_3^- or CO_3^{2-} , depending on pH), the last mainly due to subsequent co-precipitation with the Ca^{2+} and Mg^{2+} . The effect of the precipitation on inorganic carbon compared to reversible reactions was small. There is no C-ISM at the Karlsruhe-S (ND) research site.

The evolving solutions (initially Solution 0) of Robinson and Akeley C- ISMs were further treated with the mineral phases using their respective SI values. The SI values were calculated from the water samples of the chosen target solutions. The mass transfer observed ranged from 0.10 mmol/L to 1.0 mmol/L. Forward modeling ended here for the C-ISMs and validation of modeling results followed.

There is a close match between the modeled and measured values of pH in both the Robinson (ND) and Akeley (MN) C-ISMs (Fig. 13b and Fig. 14b). In general, modeled and measured Ca^{2+} , Mg^{2+} and K^+ for the control chambers are in good agreement in Robinson (ND) and were even better matched for the Akeley (MN) site (Fig. 13a and Fig. 14a, respectively).

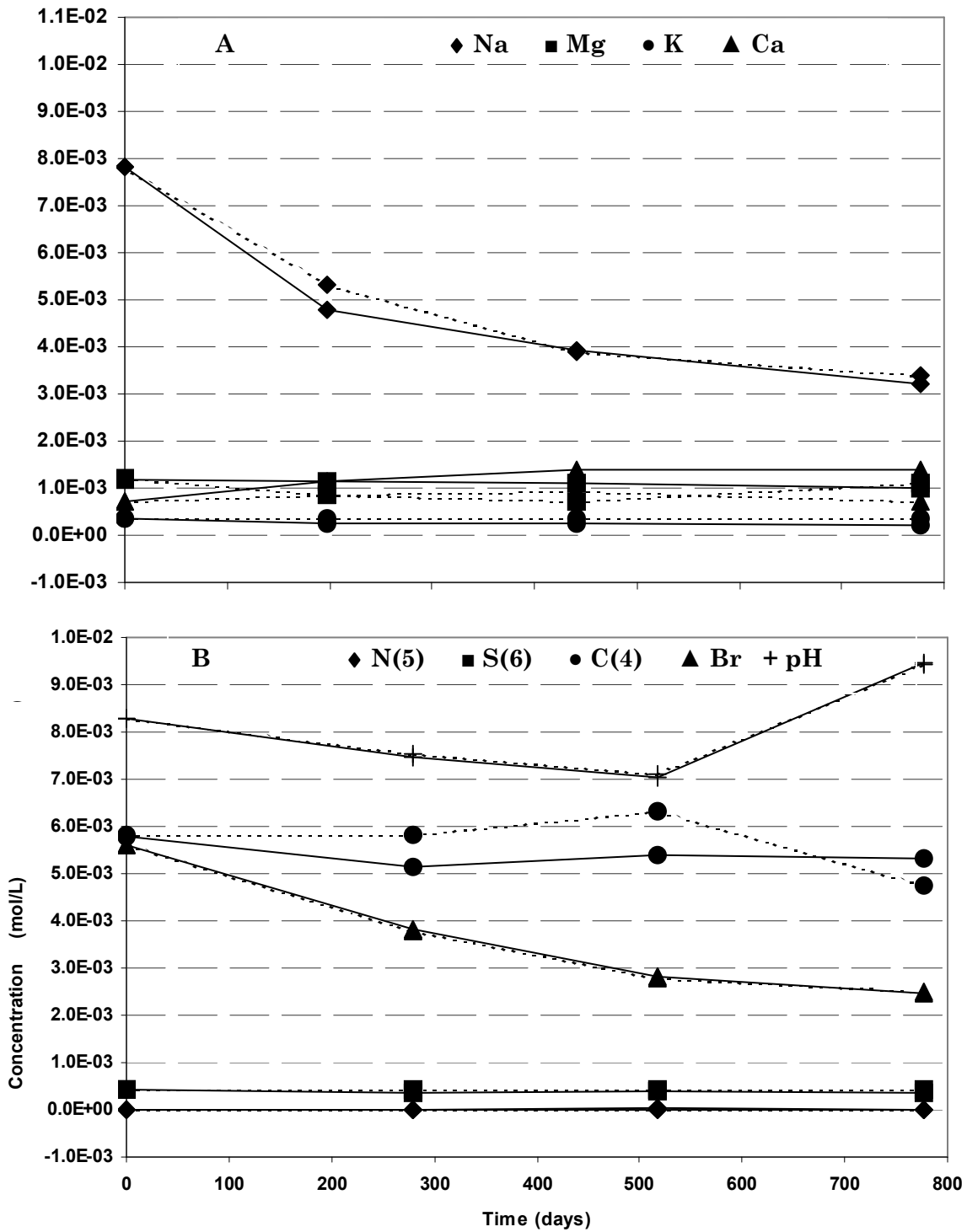


Figure 13. Modeled (dashed line) vs. Measured (solid line) Cations (A) and Anions (B), Robinson Control Chamber, ND. [pH x 10E-03].

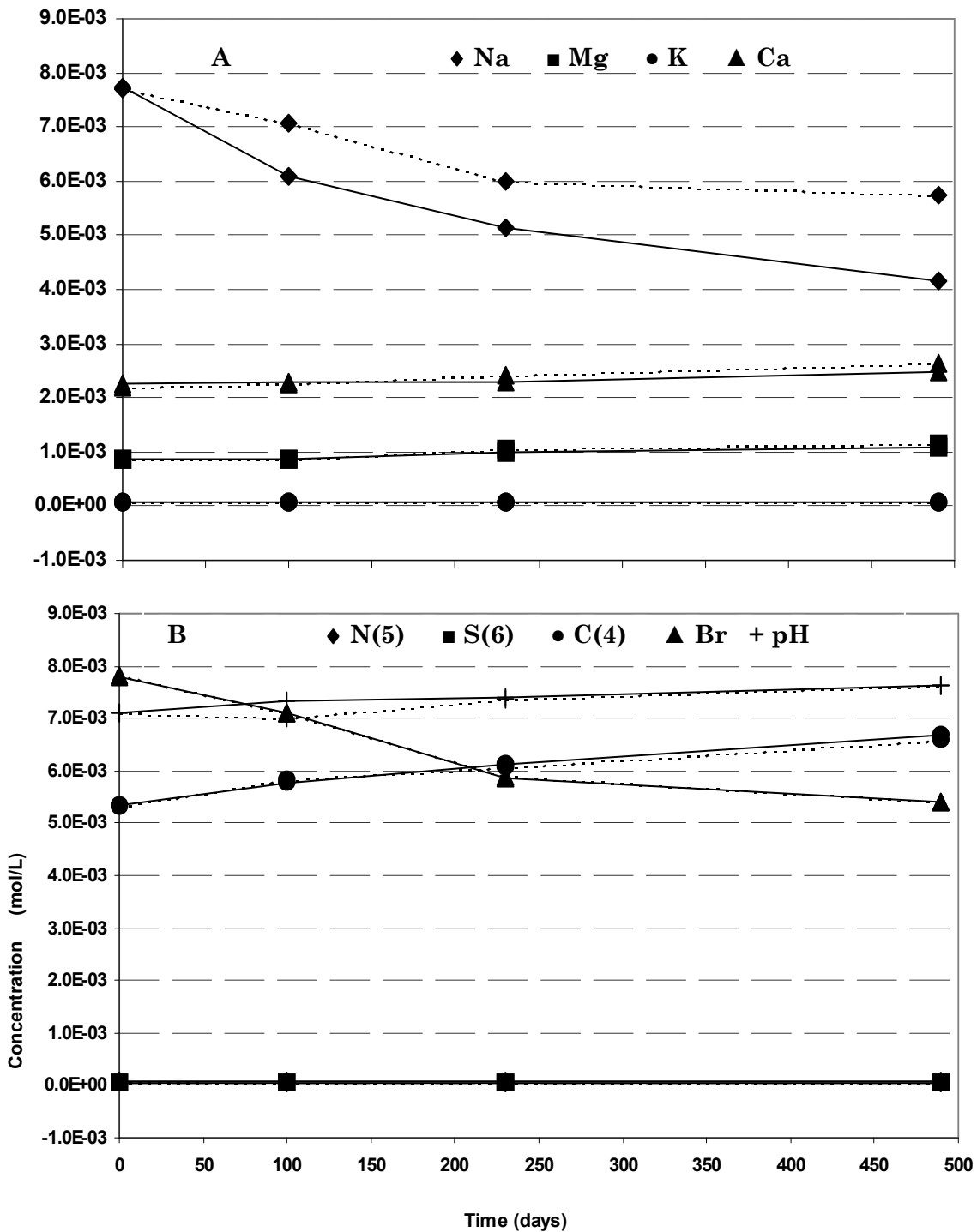


Figure 14. Modeled (dashed line) vs. Measured (solid line) Cations (A) and Anions (B), Akeley Control Chamber, MN. [pH x 10E-03].

The match for Na^+ , which was injected with the tracer Br^- , was better matched at the Robinson site; however the decreasing trend of Na^+ at the Akeley was simulated. Anions have much better coherence between modeled and measured values in both control chambers, while C(4) of Robinson displayed some irregularities. However, its apparent role in the Robinson N-ISM denitrification reactions was limited.

Recalling the challenge of simulating the complex natural geochemical environment with a relatively simple thermodynamic model, the above observations are satisfactory. Hence, validation and interpretation of the modeling results demonstrate that dilution, CEC, and reversible reactions were apparently responsible for the geochemical evolution observed for the C-ISMs. As expected, redox reactions did not seem to have any significance in the C-ISMs; however, they did in the N-ISMs.

Nitrate Chamber (N-ISM)

In addition to dilution, cation exchange reactions, and reversible reactions, redox reactions also occurred inside the N-ISMs. The major reduced species of the aquifer, as detected by various analytical measurements, are organic carbon, inorganic sulfide and Fe(II), while the oxidant of interest is nitrate. Therefore, denitrification reactions were the only redox reaction in the N-ISMs modeled. Solutions of time steps T80, T329, and T506 for Akeley, T252, T491, and T750 for Robinson and T86, T177, and T273 for Karlsruhe-S (all in days) were selected as target solutions for the forward modeling of the N-ISMs. The non-specific CEC determined for Akeley (MN) site, obtained through PHREEQC modeling, was 1.87 mmoles. As was case in the control chambers, no CEC reactions were observed in the N-ISM for Robinson and Karlsruhe-S sites. Likewise, reversible reactions were simulated using the respective saturation indices of the actual samples previously chosen as target solutions. Then, the progressively-evolved solutions were forced to react with the three electron donors, based on the methodology explained previously. The role of each electron donor varied during the course of the tracer test period. In general, the ranges and average value given in Table 5 were deduced from the “REDOX REACTION” modeling exercise (Fig. 15).

Table 5. Relative Roles of the Common Reductants in Aquifer Denitrification Reactions for Akeley (MN), Robinson (ND) and Karlsruhe-S (ND)

Research Site	Electron Donors	OC %	FeS₂ %	Fe(II) %
Akeley (MN)	Range/Average in %	46 – 60/51.2	3.0 – 14/7.47	27 – 50/41.3
Robinson (ND)	Range/Average in %	0.0 – 23/7.81	1.0 - 5.0/2.31	75 – 99/89.9
Karlsruhe-S (ND)	Range/Average in %	23 – 27/25.1	14 – 28/21.4	46 – 63/53.5

Overall results of the modeling work and estimation of the electron donors involved in the aquifer denitrification reactions are given here for Akeley (MN), Robinson (ND) and Karlsruhe-S (ND) and for the remaining sites are not included here.

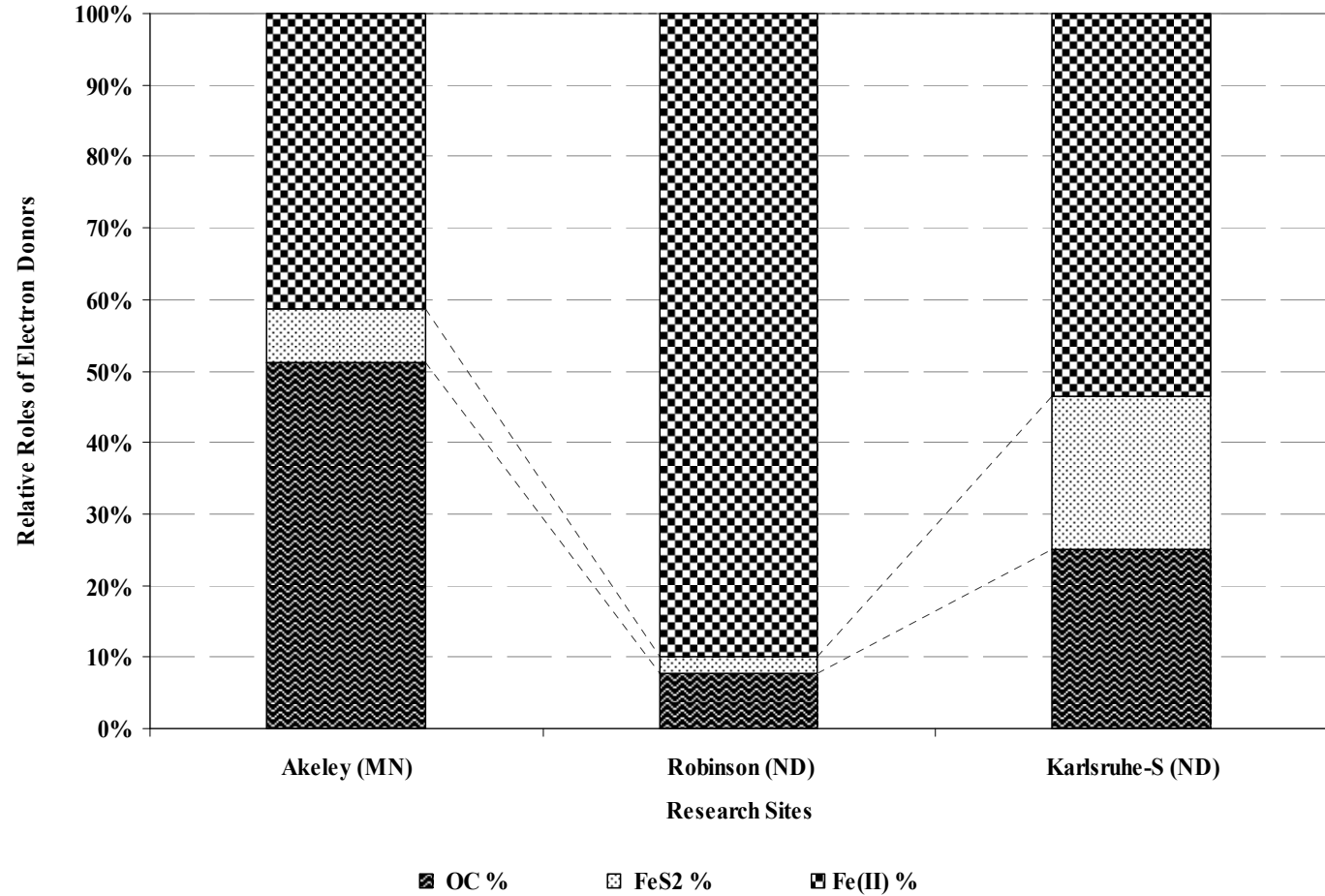


Figure 15. Average Contribution of Each Electron Donor in the Natural Denitrification Reactions of North Dakota and Minnesota Aquifers, as Computed via Advanced Geochemical Modeling, PHREEQC; Employing the Concept of Partial Geochemical Modeling (Akeley, Robinson and Karlsruhe-S)

Organic carbon and pyrite supported denitrification reactions gave rise to dissolved reaction products, inorganic carbon and sulfate, respectively. Whereas, incongruent oxidative dissolution of Fe(II)-rich silicate phases result in other secondary solid phases. Goethite, quartz, and kaolinite are the most probable reaction products for the Fe(II)-supported denitrification reactions.

Finally, validation and interpretation of modeling results was conducted using the target solutions. During such work emphasis was given to the modeled and measured cations, anions and pH values. Cations matched in all three of the sites; however, Robinson cations matched best (Fig. 16 A) followed by Akeley (Fig. 18 A). Karlsruhe-S cations displayed some irregularities but generally the deviation of the modeled from the measured values is small (Fig. 17 A). As expected Na^+ , the cation associated with the tracer Br^- , showed some deviations. Measured and modeled anions, except some minor deviation in Robinson (Fig. 16 B), matched well in Karlsruhe-S (Fig. 17 B) and Akeley (Fig. 18 B) ISMs. Measured and modeled pH values matched well in Akeley, while in Robinson they displayed irregularities.

The greatest difference between measured and modeled pH values is observed in Karlsruhe-S. In general, pH is hard to predict and differences as high as 3 pH units between modeled and measured values were observed in a previous aquifer denitrification study (Postma et al., 1991). The close matches between the modeling output and the analytical data for Akeley, Robinson and Karlsruhe-S, confirm that the major processes responsible for the geochemical evolution of the nitrate chamber were dilution, CEC, reversible reactions and denitrification reactions that involve CH_2O , FeS_2 and Fe(II) (Figures 16 - 18).

During the verification of the forward reaction modeling results, the effect of excluding CH_2O and Fe(II)-amphibole was investigated separately.

Inorganic carbon and pH were responsive to the new changes. Accordingly, when the net nitrate was forced to react with pyrite and CH_2O only, excluding Fe(II)-amphibole, large deviation between the modeling output and measured values of inorganic carbon and pH were observed. Similarly, significant discrepancies were observed between modeled and measured results of inorganic carbon and pH during the reaction simulation of net nitrate with pyrite and Fe(II)-amphibole only. Robinson and Karlsruhe-S ISM sites were more sensitive than Akeley ISM to the omission of either CH_2O or Fe(II)-amphibole.

During the forward modeling the effect of temperature and pH was investigated. Field measured temperatures of some of the ISMs ranged from 6 to 10 °C; however, it did not have a significant effect on the geochemical processes of the mesocosms. Nevertheless, pH had a significant effect on the geochemical processes of the ISMs. Lowering pH values enhanced the oxidative dissolution of the Fe(II)-rich silicate minerals. This observation

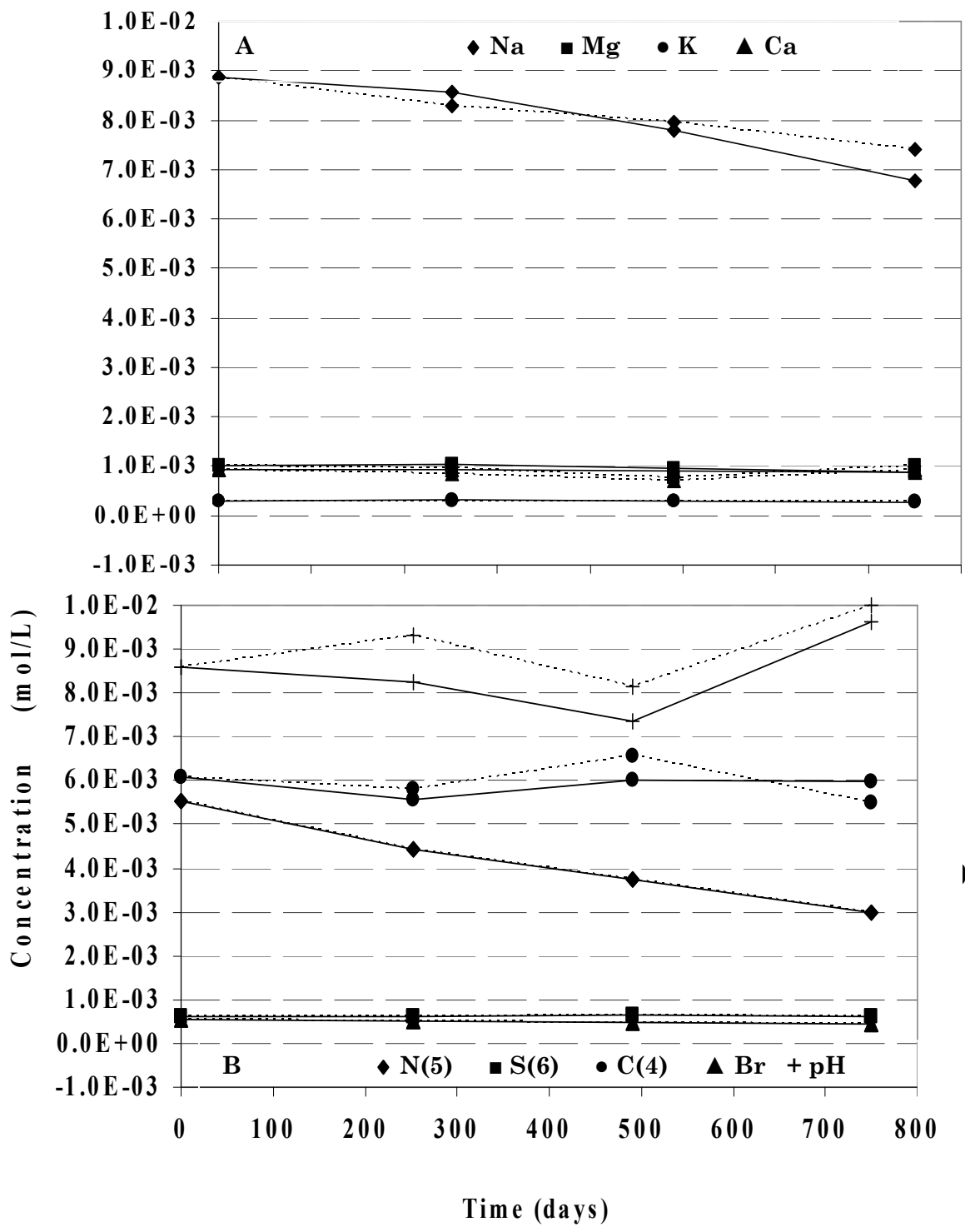


Figure 16. Modeled (dashed line) Vs Measured (solid line) Cations (A) and Anions (B) Robinson Nitrate Chamber, ND. [pH x 10E-03]

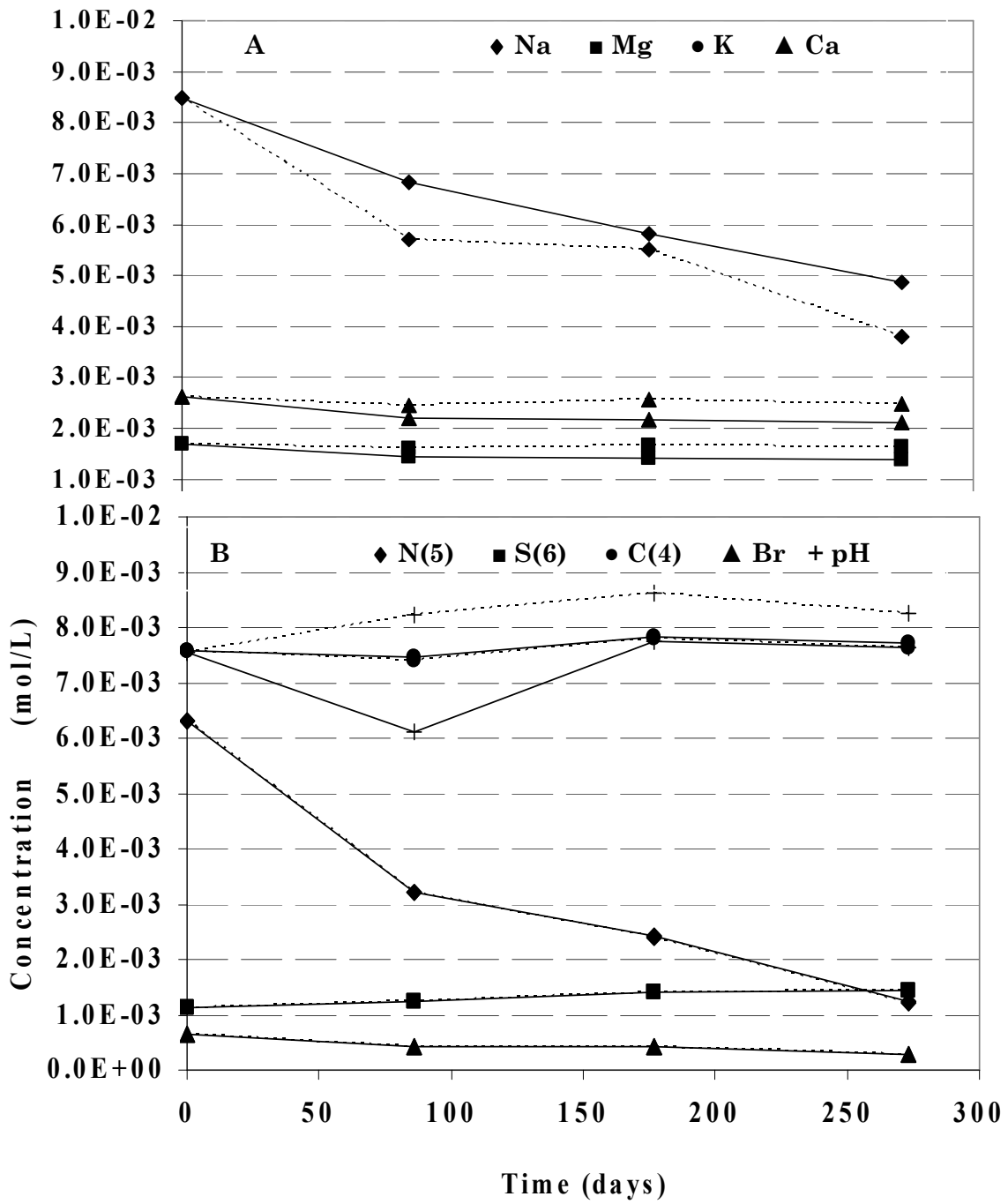


Figure 17. Modeled (dashed line) Vs Measured (solid line) Cations (A) and Anions (B) Karlsruhe-S Nitrate Chamber, ND. [pH x 10E-03].

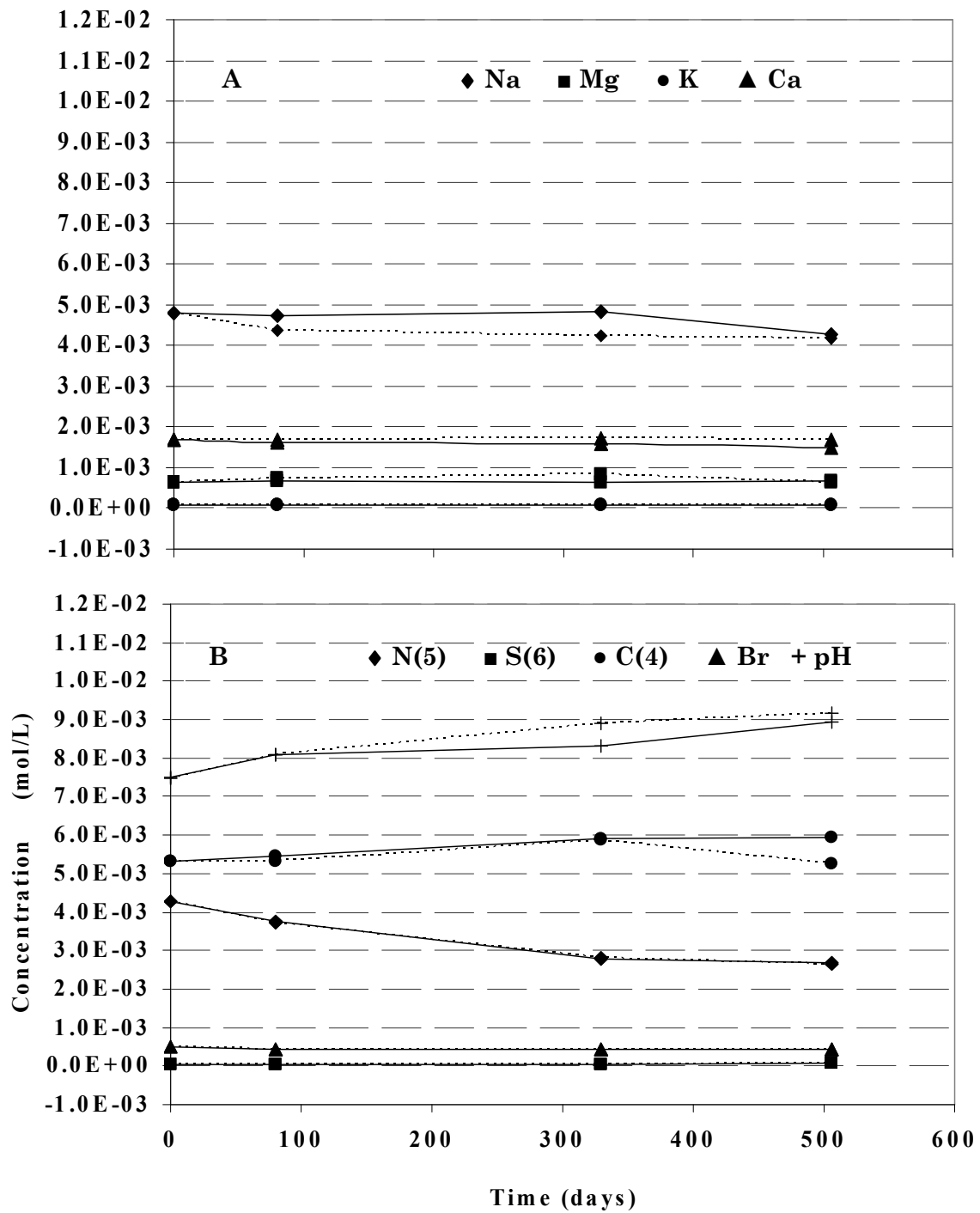


Figure 18. Modeled (dashed line) Vs Measured (solid line) Cations (A) and Anions (B) Nitrate Chamber, MN. [pH x 10E-03]

has an important implication: in open systems where the aquifers are exposed to the circulation of atmospheric gases, such as O₂, CO₂, and N₂, pH may vary and cause a change of the rate of the reactions.

It was also observed that the time needed to regain the equilibrium, which was perturbed due to the injection of nitrate to the ISM, was shorter for those sites with high concentration of electron donors and vice versa. For example, essentially 90% from the Karlsruhe-S ISMs were lost after 273 days. This site is relatively abundant in electron donors as confirmed by wet chemical extractions (Fig 4). However, in the Akeley and Robinson ISMs, sites that have relatively moderate electron donor concentrations (Fig 4), 506 days and 750 days were required to denitrify about 50% of the amended nitrates, respectively.

Conclusions

The major reasons that led to the ignorance of the role of Fe(II) in previous regional studies were two: 1) The fact that geochemical evidences for Fe(II)-supported denitrification is hard to comprehend and, 2) in the event where both inorganic carbon and Fe(III)-oxyhydroxides were precipitating, the role of Fe(II) was masked by that of the organic carbon. Therefore, two important measures were taken to tackle these problems.

First, the abundance of Fe(II) and the minerals that host it were determined using multiple complementary analytical techniques: wet chemical extractions, x-ray diffraction and Mössbauer spectroscopy. The results of these analyses confirmed that the sites where pyrite and organic carbon did not seem to be dominant are found to be relatively rich in ferrous iron minerals.

Then PHREEQC was used to resolve the intricacies between the two precipitating denitrification reaction products. First, PHREEQC simulated the amount of inorganic carbon precipitated out from solution indirectly through the co-precipitating Ca²⁺ and Mg²⁺ that were released into solution by cation exchange reactions. In some of the sites, Ca²⁺ and Mg²⁺ also decreased in solution. Therefore, computing the mass balance of Ca²⁺ and Mg²⁺ provided the maximum fraction of these cations lost from both the solid phase and solution. If all these cations were assumed to be co-precipitated together with the inorganic carbon, which is not likely, it provides the upper limit for the inorganic carbon that was possibly produced in the N-ISMs. By process of elimination the net nitrate lost due to denitrification, but not accounted for by reactions with pyrite and organic carbon, was attributed to Fe(II) and substantiated by the subsequent evolution on the water in the N-ISMs.

Validation of the modeling work by comparing output files with the target solutions of different time steps demonstrated that dilution, CEC, and reversible reactions were apparently responsible for the geochemical evolution observed in the C-ISMs. Whereas for the N-ISMs, in addition to dilution, CEC, and reversible reactions, denitrification reactions involving FeS₂, CH₂O, and Fe(II)-amphibole were the main processes influencing the geochemical environment of the N-ISMs. Therefore, all aqueous analytical data, mineralogy and chemistry of sediments and geochemical modeling works are evidently showing the proportional role of the common electron donors (Fig. 17) and Fe(II)-supported denitrification has a significant role as a natural remediation process.

Moreover, observation of the hydrochemical data of the ISMs also demonstrated that denitrification rates were higher for those sites with higher concentrations of electron donors and vice versa.

Acknowledgments

We are grateful to the North Dakota Water Resources Research Institute funded by the United States Geological Survey, the North Dakota State Water Commission (NDSWC), and the North Dakota Department of Health for their financial assistance throughout the project. I want to thank Dr. Kanishka Marasinghe, Dept. of Physics (UND) and Mr. William Schuh (NDSWC) for providing research facilities and equipment.

References

- Afzal, B. (2006). Drinking water and Women's health. *Journal of midwifery and women health*, v. 51, issue 1, 12-18.
- [ASTM] American Society for Testing and Materials. (1993). Construction, section 4, soil and rock; dimension stone; geosynthesis. In *Annual Book of ASTM Standards*, vol. 04.08. Philadelphia, Pennsylvania: American Society for Testing and Materials.
- Amin, M., Abbaspour, C. K., Khademi, H., Fathianpour, N., Afyuni, M., and Schulin, R. (August 2005). Neural network models to predict cation exchange capacity in arid regions of Iran. *European Journal of Soil Science*, 56, 551–559.
- Appelo, C.A.J., and Postma, D. (1996). *Geochemistry, groundwater and pollution*. A.A. Balkema, Rotterdam. p. 275.
- Barton, C.D., and Karathanasis, A.D. (1997). Measuring cation exchange capacity and total exchangeable bases in batch and flow experiments. *Soil Technology* 11, 153-162.
- Benz, M., Brune, A., and Schink, B. (1998). Anaerobic and aerobic oxidation of ferrous iron at neutral pH by chemoheterotrophic nitrate-reducing bacteria. *Arch Microbiol* 169:159–165.
- Bethke, C.M. (1996). *Geochemical Reaction Modeling*, Oxford U.P., New York.
- Blicher-Mathiesen, G., McCarty, G. W. and Nielsen, L. P. (1998). Denitrification and degassing in groundwater estimated from dissolved dinitrogen and argon. *J. Hydrol.* 208: 16-24.
- Böhlke, J.K., Wanty, R., Tuttle, M., Delin, G., and Landon, M. (2002). Denitrification in the recharge area and discharge area of a transient agricultural nitrate plume in a glacial outwash sand aquifer, Minnesota: *Water Resources Research*, v. 38(7), 10.1029/2001WR000663, 200238, p. 10.1-10.26.
- Bradley, Edward, Petri, R. L. and Adolphson, G. D. (1963). *Geology and Ground Water Resources of Kidder County, North Dakota, Ground Water and Chemical Quality of Water, Part III*, 38 p.
- Breeuwisma, A., Wösten, J.H.M., Vleeshouwer, J.J., Van Slobbe, A.M., and J. Bouma. (1986). Derivation of land qualities to assess environmental problems from soil surveys. *Soil Sci. Soc. Am. J.* 50:186–190.
- Canfield, D.E., Raiswell, R., Westrich, J.T., Reaves, C.M., and Berner, R.A. (1986). The use of chromium reduction in the analysis of reduced inorganic sulfur in sediments and shales, *Chemical Geology*, 54(1/2), 149-155.
- Churcher, P.L., and Dickout, R.D. (1987). Analysis of ancient sediments for total organic carbon-Some new ideas. *Journal of Geochemical Exploration* 29, no. 2: 235–246.
- Cowdery, T.K., (1997). *Shallow ground-water quality beneath cropland in the Red River of the North Basin, Minnesota and North Dakota, 1993-95*. U.S. Geological Survey.
- Dane, H. Jacob, and Topp, G. Clarke (ed.). (2002). *Soil Science Society of America Book Series*, no. 5. *Methods of Soil Analysis. Part 4. Physical Methods*. Soil Science Society of America, Inc., Madison, WI.
- Devlin, F. J., Eedy, R., and Butler, J. B. (2000). The effects of electron donor and granular iron on nitrate transformation rates in sediments from a municipal water supply aquifer. *Journal of Contaminant Hydrology* 46, 81–97

- Dyar, M.D. and Scafer, M.W. (2004), Mössbauer spectroscopy on the surface of Mars: constraints and expectations. *Earth and Planetary Science Letters* 218, 243-259.
- Ernstsen, V. (1996). Reduction of nitrate by Fe²⁺ in clay minerals. *Clays and Clay Minerals* 44: 599-608.
- Fetter, C.W. (1994). *Applied Hydrogeology* (4th edition). Prentice-Hall, Upper Saddle River, New Jersey, 598 pages.
- Firestone, M. K. (1982). Biological denitrification, in *Nitrogen in Agricultural Soils*, edited by F. J. Stevenson, American Society of Agronomy, Madison, Wisconsin, 289-326.
- Gillham, R.W., and Cherry, J.A. (1978). Field evidence of denitrification in shallow ground water flow systems. *Water Pollution Research in Canada* 13:53-71.
- Hach Company Web Site, http://www.hach.com/wateranalysis/handbook/english/eng_i.htm.
- Hartog N., J. Griffioen and P.F. van Bergen. (2005). "Depositional and Paleohydrogeological Controls on the Distribution of Organic Matter and Other Reactive Reductants in Aquifer Sediments" *Chemical Geology*. 216(1-2) pp. 113-131.
- Hauck, S., Benz, M., Brune, A., and Schink, B. (2001). Ferrous iron oxidation by denitrifying bacteria in profundal sediments of a deep lake (Lake Constance). *FEMS Microbiol. Ecol.* 37: 127–134.
- Hawthorne, F. C. (1983). Quantitative characterization of site-occupancies in minerals. *Am. Mineral.* 68, 287pp.
- Heath, R. C. (1984). *Groundwater Regions in the United States*. U. S. Geological Survey Water-Supply Paper, 2242.
- Heron, G. Crouzet, Bourg, C., and Christensen, A.C.M. (1994). Speciation of Fe (II) and Fe (III) in contaminated aquifer sediments using chemical extraction techniques. *Environm. Sci. Technol.* 28, 1698-1705.
- Heron, G., and T. H. Christensen. 1995. Impact of sediment-bound iron on redox buffering in a landfill leachate polluted aquifer (Vejen, Denmark). *Environ. Sci. Technol.* 29:187–192.
- International Centre for Diffraction Data. (2002). XRD machine built-in database.
- Kalinowski, B.E., Liermann, L. J., Givens, S., and Brantley, S.L. 2000. Rates of bacteria-promoted solubilization of Fe from minerals: A review of problems and approaches. *Chemical Geology*, 169, 357-370.
- Kammer, A.E. (2001). Laboratory denitrification using sediment from the Elk Valley aquifer. M.S. thesis, Department of Geology & Geological Engineering, University of North Dakota, Grand Forks, North Dakota.
- Kehew, A.E. (2001). *Applied Chemical Hydrogeology*. Prentice-Hall, Inc., 368p.
- Kennedy, L.G., Everett, J. W., Ware, K. J., Parsons, R., and Green, V. (1999). Iron and sulfur mineral analyses methods for natural attenuation assessments. *Bioresour. J.* 2, 259-276.
- Korom, S.F. (1992). Natural denitrification in the saturated zone: A review. *Water Resources Research* 28, no. 6: 1657–1668.
- Korom, Scott F. (2005). *Assessment of Denitrification Capabilities in North Dakota Aquifers*, Section 319 Final Project Report.
- Korom, Scott F., Schlag, Allen J., Schuh, William M., and Kammer Schlag, Alison. (2005). In situ mesocosms: Denitrification in the Elk Valley aquifer. *Ground Water Monitoring & Remediation* 25 (1), 79-89.
- Lalonde, E. A., Rancourt, G. D., and Ping, Y. J. (1998). Accuracy of ferric/ferrous determinations in micas: A comparison of Mössbauer spectroscopy and the Pratt and Wilson wet-chemical methods. *Hyperfine Interactions* 117, 175–204.
- Liermann, L., Barnes, A.S., Kalinowski, B.E., Zhou, X., and Brantley, S.L. (2000). Microenvironments of pH in biofilms grown on dissolving silicate surfaces. *Chemical Geology*, 171, 1-16.
- Lindgren, J. R., and Landon, M. K. (2000). Effects of ground-water withdrawals on the Rock River and associated valley aquifer, eastern Rock County, Minnesota. Prepared in cooperation with the Minnesota Department of Natural Resources; the City of Luverne, Minnesota; and the Rocky County Rural Water District. 103p.
- Linge, K.L. (1996). Iron speciation in an aquifer contaminated by hydrocarbons. Department of Chemistry, University of Western Australia. Unpublished honours thesis.
- Lovley, D.R., and Phillips, E.J.P. (1986a). Availability of ferric iron for microbial reduction in bottom sediments of the freshwater tidal Potomac river. *Appl. Environ. Microbiol.* 52 (4), 751-757.
- Lovley, R. D. and John D Coates, D, J. (2000). Novel forms of anaerobic respiration of environmental relevance. *Current Opinion in Microbiology*, 3:252–256.

- Manassaram, Deana M., Backer, Lorraine C., and Moll, Deborah M. A Review of Nitrates in Drinking Water: Maternal Exposure and Adverse Reproductive and Developmental Outcomes. *Environmental Health Perspectives* Volume 114, Number 3, March 2006.
- McCammon, Catherine. (1995). Mössbauer spectroscopy minerals. American Geophysical Union.
- McKeon, C., Glenn, E. P., Jordan, F., Waugh, W. J., and S. G. Nelson. (2005). "Rapid nitrate and ammonium loss from a contaminated desert soil." *Journal of Arid Environments* 61:119-136.
- Miller, R. H. Page, A.L., Keeney, D.R., Baker, D. E., Roscoe Ellis, J., and Rhosdes, D. J. (1982). *Methods of soil analyses, part 2, chemical and microbiological properties, 2nd edition*, Madison, Wisconsin, pp. 300-312.
- Mooers, H.D. and Norton, A.R. (1997). Glacial landscape evolution of the Itasca/St. Croix moraine interlobate area including the Shingobee river headwaters area. In winter, T.C., editor, *Hydrological and biogeochemical research in the Shingobee river headwaters area, north-central Minnesota*. Denver CO: U.S. Geological Survey, 3/10.
- Mössbauer Spectroscopy, World Wide Web: A Powerful Tool in Scientific Research. Presentation by P. Gütlich¹, J.M. Greneche², F.J. Berry³ (<http://www.mossbauer.org/mossbauer.html>)
- Palandri, James L. and Kharaka, Yousif K. (2004). A compilation of rate parameters of water-mineral interaction kinetics for application to geochemical modeling. U.S.G.S open file report-1068.
- Parkhurst, D.L. and Appelo, C.A.J. (1999). User's guide to PHREEQC (version 2)-A computer program for speciation, batch-reaction, one-dimensional transport, and inverse geochemical calculations: U.S.G.S. *Water-Resources Investigations Report* 99-4259, 312 p.
- Poppe, L. J., Paskeich, V. F., Hathaway, J. C., and Blackwood, D. S. (2002). A laboratory manual for X-ray powder. U. S. Geological Survey Open-File Report 01-041. 88 pp.
- Postma, D. (1990). Kinetics of nitrate reduction in a sandy aquifer. *Geochimica et Cosmochimica* 54:903-908.
- Postma, D., Boesen, C., Kristiansen, H., and Larsen, F. (1991). Nitrate reduction in an unconfined aquifer: water chemistry, reduction processes, and geochemical modeling. *Water Resour. Res.* 27: 2027-2045.
- Power, J.F. and Schepers, J.S. (1989). Nitrate contamination of groundwater in North America. *Agriculture, Ecosystems, and Environment* 26:165-188.
- Prommer, H., Barry, D.A., and Davis, G.B. (1999). Geochemical changes during biodegradation of petroleum hydrocarbons: Field investigations and biogeochemical modeling. *Organic Geochemistry* 30.
- Puckett, L.J., and Cowdery, T.K. (2002) Transport and fate of nitrate in a glacial outwash aquifer in relation to ground water age, land use practices, and redox processes. *Journal of Environmental Quality*, 31(3), 782-796.
- Robertson, W.D., Russell, B.M., and Cherry, J.A. (1996). Attenuation of nitrate in aquitard sediments of southern Ontario. *J. Hydrol.* 180:267-281.
- Rodvang, S.J., and Simpkins, W.W. (2001). Agricultural contaminants in Quaternary aquitards: A review of occurrence and fate in North America. *Hydrogeol. J.* 9:44-59
- Rogers, J.R., and Bennett, P.C. (2004). Mineral stimulation of subsurface microorganisms--Release of limiting nutrients from silicates: *Chemical Geology*, v. 203, no. 1-2, p. 91-108, doi:10.1016/j.chemgeo.2003.09.001.
- Royal Society of Chemistry Website <http://www.rsc.org>.
- Schlag, A. J., (1999). In-site measurements of denitrification in the Elk Valley aquifer, M.S. thesis, 104 pp., University of North Dakota, Grand Forks, ND.
- Schröder, I., Johnson, E., and Vries, S. (2003). Microbial ferric iron reductases. *FEMS Microbiology Reviews* 27, 427-447.
- Schultz, A.P., Milici, R.C., Bartholomew, M.J., Levan, D.C. and Wilkes, G.P. (1980). *Geologic Structure and Hydrocarbon Potential along the Saltville and Pulaski Thrusts in Southwestern Virginia and Northeastern Tennessee*: Virginia Division of Mineral Resources Publication 23.
- Senn D.B., and Hemond, H.F. (2002). Nitrate controls on iron and arsenic in an urban lake. *Science*, vol. 296:2373-2376.
- Shelobolina, E.S., Gaw VanPraagh, C.V., and Lovley, D.R. (2003). Use of Ferric and Ferrous Iron Containing Minerals for Respiration by *Desulfitobacterium frappieri*, *Geomicrobiol J.* 20:143-156.
- Skubinna, P. A. (2004). Modeling the hydrogeochemistry of denitrification in the Elk Valley M.S. thesis, 145 pp., University of North Dakota, Grand Forks, ND.
- Sobolev, D., and Roden, E. (2002). Evidence for rapid microscale bacterial redox cycling of iron in circumneutral environments. *Antonie van Leeuwenhoek* 81:587-597.

- Spencer, E. (2005). Isotopic Tracers as Evidence of Denitrification in the Karlsruhe Aquifer. M.S. thesis, University of North Dakota, Grand Forks, ND.
- Starr, R.C., and Gillham, R.W. (1993). Denitrification and organic carbon availability in two aquifers. *Ground Water* 31:934-947.
- State of North Dakota Water Commission Website
<http://www.swc.state.nd.us/4DLink2/4dcgi/WellSearchForm>
- Straub K.L., Benz M, Schink B, and Widdel, F. (1996). Anaerobic, nitrate-dependent microbial oxidation of ferrous iron. *Appl Environ Microbiol* 62:1458–1460.
- Straub, K.L., Benz, M., and Schink, B. (2001). Iron metabolism in anoxic environments at near neutral pH. *FEMS Microbio/ Eco/34*: 181-186.
- Stoner, J.D., Lorenz, D. L., Wiche, G. J. and Goldstein, R. M. (1993). Red River of the North Basin, Minnesota, North Dakota, and South Dakota. *Water Resources Bulletin* vol. 29, no. 4.
- Teller, J.T., and Kehew, A.E., (1994). Introduction to the late glacial history of large proglacial lakes and meltwater runoff along the Laurentide Ice Sheet: *Quaternary Science Reviews*, v. 13, p. 795-799.
- Tesoriero, A.J., Liebscher, H., and Cox, S.E. (2000). The mechanism and rate of denitrification in an agricultural watershed: Electron and mass balance along ground water flow paths. *Water Resour. Res.* 36:1545–1559.
- Trudell, M. R., Gillham, R. W., and Cherry, J. A. (1986). An in-situ study of the occurrence and rate of denitrification in a shallow unconfined sand aquifer, *Journal of Hydrology*, 83(3/4), 251-268.
- Tuccillo, M.E., Cozzarelli, I.M., and Herman, J.S. (1999). Iron reduction in the sediments of a hydrocarbon-contaminated aquifer: *Applied Geochemistry*, v. 14, no. 5, p. 71-83.
- U.S. Environmental Protection Agency World Wide Web
http://www.epa.gov/OGWDW/methods/inch_tbl.html
- U. S. Geological Survey World Wide Web: Map showing the thickness and character of Quaternary sediments in the glaciated United States east of the Rocky Mountains: Surficial Quaternary sediments
<http://pubs.usgs.gov/dds/dds38/metadata.html>
- U.S. G. S. Map of Surficial Geology and Contamination (Online Map)
<http://www.deq.state.mi.us/documents/deq-ogs-land-gmc-bookdown.pdf#search='Map%2C%20Nitrate%20and%20Glaciated%20sediments'>.
- U.S. Geological Survey. (2000). Water-Resources Investigations Report 00-4219. Online document, Tallahassee, Florida http://fl.water.usgs.gov/PDF_files/wri00_4219_katz.pdf.
- Van Kessel, J. F. (1977). Removal of nitrate from effluent following discharge on surface water. *Water research* 11: 533-537.
- Warne, J. (2004). Design and Evaluation of a Modified In Situ Mesocosm to Study Denitrification in the Karlsruhe Aquifer. M.S. thesis, University of North Dakota, Grand Forks, ND.
- Weber, K. A., Picardal, F. W., and Roden, E. E. (2001). Microbially Catalyzed Nitrate-Dependent Oxidation of Biogenic Solid-Phase Fe(II) Compounds. *Environ. Sci. Technol.* 35(8), 1644-1650.
- Wikipedia online Encyclopedia; <http://en.wikipedia.org/wiki/Iron>.
- Zachara, J. M., Ainsworth, C. C., Brown, G. E., Catalano, Jr., J. G., McKinley, J. P., Qafoku, O., Smith, S. C., Szecsody, J. E., Traina, S. J., and Warner, J. A. (2004). Chromium speciation and mobility in a high level nuclear waste vadose zone plume. *Geochim. Cosmochim. Acta* 68(1), 13-20.
- Zheng, C. (2002). PHREEQC and PHREEQCI: Geochemical Modeling with an Interactive Interface. *Groundwater* v. 40, No. 5 462-464.
- Zhu, Chen, and Anderson, Gregory (2002). Environmental applications of geochemical modeling: Cambridge University Press, 284 p.